Journal of Porphyrins and Phthalocyanines
J. Porphyrins Phthalocyanines 2010; **14**: 759–792
DOI: 10.1142/S1088424610002689

Published at http://www.worldscinet.com/jpp/

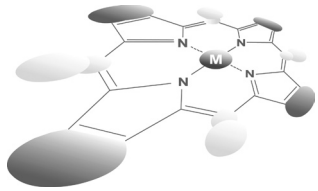

Porphyrins and phthalocyanines in solar photovoltaic cells

Michael G. Walter[a◊], **Alexander B. Rudine**[b◊◊] **and Carl C. Wamser***[b◊]

[a] *Division of Chemistry & Chemical Engineering, California Institute of Technology, Pasadena, CA 91125, USA*
[b] *Department of Chemistry, Portland State University, Portland, OR 97207-0751, USA*

Received 25 June 2010
Accepted 23 July 2010

ABSTRACT: This review summarizes recent advances in the use of porphyrins, phthalocyanines, and related compounds as components of solar cells, including organic molecular solar cells, polymer cells, and dye-sensitized solar cells. The recent report of a porphyrin dye that achieves 11% power conversion efficiency in a dye-sensitized solar cell indicates that these classes of compounds can be as efficient as the more commonly used ruthenium bipyridyl derivatives.

KEYWORDS: solar cells, dye-sensitized solar cells, photosensitizers, photovoltaics.

INTRODUCTION

Nature has chosen chlorophyll as the centerpiece of photosynthesis. Chlorophyll not only provides the brilliant green color we associate with living plants, it is also a working molecule, directly involved in all the key steps of solar energy conversion – light harvesting, energy transfer, and electron transfer [1]. Furthermore, photosynthesis is a spectacularly successful enterprise; worldwide it is estimated that total energy conversion via photosynthesis is well over 100 TW [2], dwarfing the total amount of energy used by humans (about 13 TW in 2005) [3]. It is not surprising then that scientists have expended tremendous effort at learning from natural photosynthesis and attempting to create comparably successful systems, a field often dubbed "artificial photosynthesis" [4]. In general, artificial photosynthesis implies that something has been learned or borrowed from natural photosynthesis, especially the molecules (chlorophylls and electron-transport agents) or the strategies (light harvesting by exciton delocalization and electron transport via donors and acceptors with appropriate energy levels). In this review, we will survey the solar energy applications that use porphyrins, chlorins, phthalocyanines, and some closely related macrocycles. We will restrict the review to solar photovoltaic cells, recognizing that there is a parallel growing literature in which these compounds are also being used as catalysts for solar chemistry, such as water splitting or CO_2 reduction [5].

Basic aspects of solar energy conversion

Photovoltaic cells require an extended sequence of successful photophysical processes in order to efficiently convert sunlight into electrical energy. The fundamental sequence is as follows: light absorption generates an electronically excited state, the excited state must either appear at or migrate to an interface or heterojunction where an electron transfer can take place, then the oxidized and reduced species (holes and electrons) must be able to migrate to opposite sides of the cell where they can be collected as electrical energy. A typical solar cell thus needs at least three key components: a light-absorber (dye), a hole-transport agent, and an electron-transport agent. Sometimes one component is forced into multiple duties, as in a typical silicon cell, where silicon is the absorber and with different doping also serves as either a hole-transport (p-type) or electron-transport (n-type) agent. Many organic solar cells apply a similar approach, using the light-absorbing dyes as charge-transport agents, but other approaches separate all three functions to different materials.

The first requirement is the harvesting of a significant fraction of the solar spectrum. Roughly half the total energy of sunlight appears at wavelengths below 700 nm, a region typically covered well by the porphyrin and

◊SPP full and ◊◊student member in good standing

*Correspondence to: Carl C. Wamser, email: wamserc@pdx.edu

Copyright © 2010 World Scientific Publishing Company

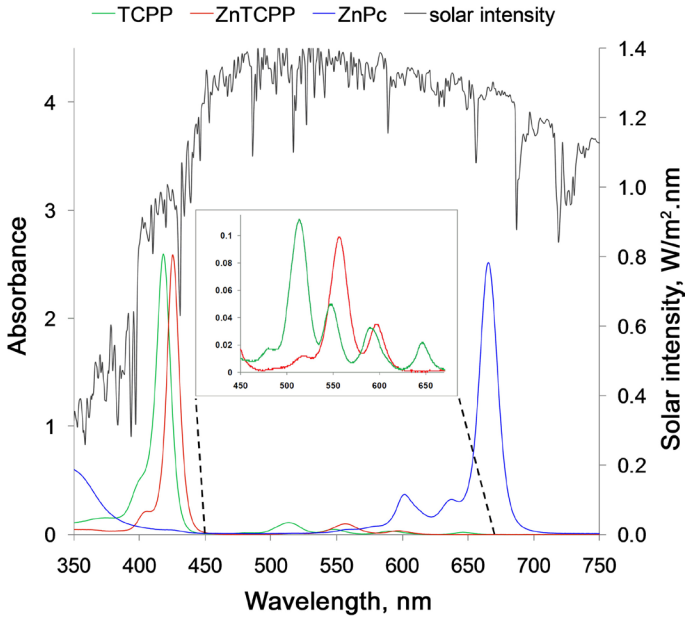

Fig. 1. Normalized absorption spectra of typical tetrapyrroles and the spectrum of solar irradiance. TCPP = tetra(4-carboxyphenyl)porphyrin, ZnPc = zinc phthalocyanine; solar intensity at AM1.5 from NREL (*http://rredc.nrel.gov/solar/spectra/am1.5*)

phthalocyanine families (Fig. 1). Additional absorption at longer wavelengths can gain additional efficiencies up to a point; the theoretical optimum band gap is at about 1.1 eV (1100 nm), and the maximum efficiency is about 33% [6]. Although a smaller band gap (at longer wavelengths) allows for harvesting a larger fraction of the solar spectrum, there are diminishing returns caused by the effect of degrading higher-energy photons to the level of the decreasing band gap. Thus an ideal solar absorber would appear black – absorbing all the ultraviolet and visible and into the near infrared. Silicon is indeed tough competition, with a broad absorption out past 900 nm. Porphyrins and related derivatives having extended conjugation are a common approach to extending the range of the absorption spectrum into the near infrared.

After solar light harvesting, charge separation is the next essential step. Typically this requires an interface or heterojunction with some different material. The excited states generated upon light absorption must transfer an electron (either oxidatively or reductively) in order to generate opposite charges. The energetic requirement is that the two different materials must have offset energy levels suitable for an electron transfer rapid enough to compete with deactivation of the excited state (typically nanoseconds). The physical requirement is that the two different materials must be close enough for this reaction to be that rapid. Two different approaches are common here. If the light absorbing dye is bound as a monolayer to an appropriate material with suitably different energy levels, electron transfer can be fast between the two materials. This is the approach of a dye-sensitized solar cell (DSSC), which typically uses a semiconductor such as TiO_2 as an electron acceptor, decorated with monolayer coverage of a dye, most commonly ruthenium complexes but often an organic dye such as a porphyrin. The overall arrangement and energetics are summarized in Fig. 2. A DSSC is typically built upon a transparent electrode such as fluorine-doped tin oxide (F:SnO_2 or FTO) or ITO (indium-doped tin oxide). Semiconductor nanoparticles are sintered onto the transparent electrode, providing a huge surface area so that even a single monolayer coverage of dye can provide substantial light absorption. Furthermore, every light-absorbing dye molecule is directly attached to the semiconductor to optimize charge separation. Devising the specific linkages between the dye and the semiconductor is an active area of research because the linkages affect the efficiency of charge separation and/or charge recombination (the undesirable reverse reaction that simply regenerates the ground state). Completing the circuit in a DSSC is typically accomplished with a redox electrolyte, almost always iodide/triiodide. A characteristic weakness of DSSCs is this reliance on a liquid phase for diffusive electron transport. There are widespread efforts to create a solid-state DSSC.

An alternative approach to controlling photoinduced charge separation is the bulk heterojunction (BHJ) cell. A BHJ cell typically consists of an intimate (usually nanostructured) blend of two different materials, such that light absorption by either component generates excited states close to an interface, where charge separation can take place (Fig. 3). A key requirement here is the ability of excited states to move to the nearest interface successfully. A mobile excited state in a uniform material is called an exciton. Excitons have short lifetimes similar to

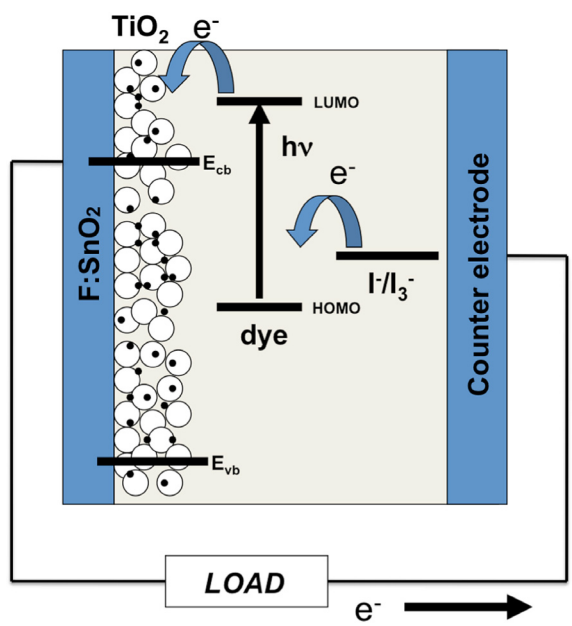

Fig. 2. The components and electron transfer processes in a typical dye-sensitized TiO_2 solar cell

Copyright © 2010 World Scientific Publishing Company

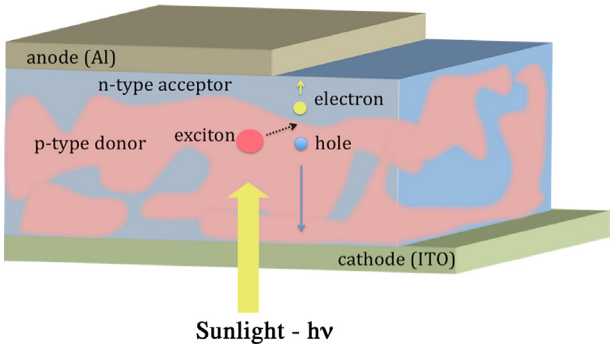

Fig. 3. Exciton migration and charge separation in a bulk heterojunction (BHJ) cell

those of excited states, and therefore they cannot diffuse very far before collapsing back to the ground state. Typical exciton diffusion lengths in organic materials are on the order of 10 nm. Thus a BHJ cell must have all light absorbers within about 10 nm of an interface, requiring either carefully nanostructured or intimately blended materials. Extending exciton diffusion lengths by careful organization, as nature does with photosynthetic antenna systems, is an area of active research [7, 8].

Finally, the separated charges (oxidized and reduced equivalents, or holes and electrons) must be able to migrate substantial distances (typically a few micrometers at least) to be collected at the opposite electrodes; from there the rest is electrical engineering. But getting charges through organic materials is problematic; electron and hole mobilities are low for most organic compounds. Hence conductive polymers are of particular interest. For example, polythiophenes and poly(phenylenevinylenes) are common constituents of BHJ cells [9]. DSSCs typically use an inorganic semiconductor (TiO_2) to transport electrons and a liquid-phase redox system (I^-/I_3^-) to shuttle holes [10]. Porphyrins and derivatives organized as liquid crystals [11] or as conductive nanostructured polymers [12] have been studied as improved charge carrier materials for solar cells.

Solar energy conversion efficiencies

Solar efficiency can be measured as a quantum yield, ϕ (number of electron/hole pairs collected per absorbed photon, sometimes called internal quantum efficiency, IQE) or as an incident-photon-to-current efficiency (IPCE, number of electron/hole pairs collected per incident solar photon, sometimes called external quantum efficiency, EQE). Both of these efficiency measures are functions of the wavelength of the incident light, and the ratio of the two is a measure of the efficiency of light absorption (which can be determined independently based on the absorption spectrum). Efficiency as a function of wavelength is typically called an action spectrum.

A more comprehensive efficiency measure is the overall power conversion efficiency (η), sometimes called PCE, which compares the total electrical energy output

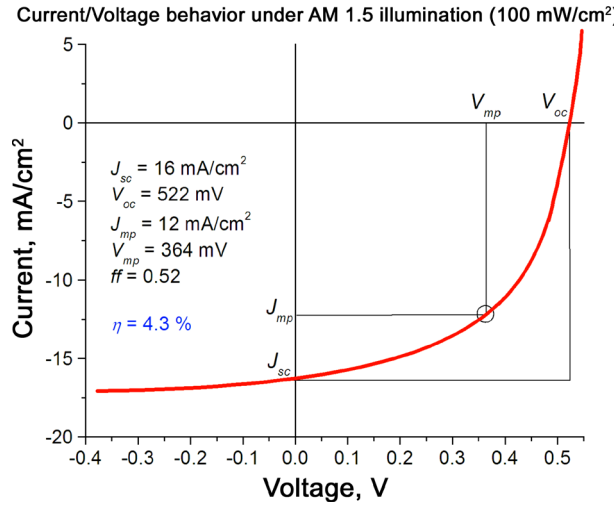

Fig. 4. A photocurrent-voltage curve for a hypothetical solar cell, illustrating points for short circuit, open circuit, and maximum power

with the total energy contained in the solar irradiance. A standard solar irradiance is typically taken as the integrated solar spectrum as it reaches Earth's surface after traversal of 1.5 atmosphere thickness (AM1.5 Global standard) [6]. The total energy is very close to 1 kW/m^2 or 100 mW/cm^2, a convenient value for comparing the output from a laboratory 1 cm^2 cell. All data cited in this review have been measured at AM1.5G unless otherwise noted.

Experimentally, the output of a photovoltaic cell is measured with a photocurrent-voltage (*IV*) curve (Fig. 4). A comparable curve is also determined in the dark, typically showing simple diode behavior – zero current at applied voltages until a breakdown potential is reached. Limiting cases in the photocurrent-voltage curve are the short-circuit and open-circuit conditions, where short-circuit photocurrent (I_{sc}), or more appropriately, photocurrent density (J_{sc}), is measured (with zero applied voltage) and open-circuit photovoltage (V_{oc}) is measured (with zero current). In the working cell, it is not possible to extract both the maximum current and the maximum potential; maximum power (current x voltage) is obtained at some intermediate point (J_{mp}, V_{mp}). The ideality of the cell is measured by the fill factor (*ff*), which is the fraction of the maximum power compared to the ideal power. The overall solar energy conversion efficiency is the maximum power extracted compared to the incident solar power.

$$\text{Fill Factor } ff = \frac{J_{mp} \cdot V_{mp}}{J_{sc} \cdot V_{oc}}$$

$$\text{Efficiency } \eta = \frac{J_{mp} \cdot V_{mp}}{P_{in}} = \frac{J_{sc} \cdot V_{oc} \cdot ff}{P_{in}}$$

Optimizing the output of a typical photovoltaic cell then seeks to maximize the short-circuit photocurrent, the open-circuit photovoltage, and the fill factor.

Copyright © 2010 World Scientific Publishing Company

Photocurrent is generally the most sensitive measure of the success of a photovoltaic cell. It depends on the light-harvesting efficiency (the absorption spectrum), the quantum efficiency of charge separation, and the avoidance of undesirable back reactions (effectively representing short circuits). Photovoltage is primarily determined by the choice of materials and their relative energy levels, although kinetic factors can also diminish photovoltage. Electrons enter one electrode from the lowest unoccupied molecular orbital (LUMO) of the acceptor material and holes are injected into the counter electrode from the highest occupied molecular orbital (HOMO) of the donor material. For semiconductors, LUMO and HOMO correlate with the conduction band and the valence band, respectively. Fill factor is governed primarily by cell resistances: internal shunt (parallel) resistances and series resistances. In an ideal cell, parallel resistances would be infinite (no shunts) and series resistances would be negligible. Such a cell would be an ideal diode, for which the *IV* plot would follow an exponential curve and would have a fill factor of 0.89 [9].

Because of the versatility and variability of their molecular structures, optical spectra, electrical properties, and supramolecular organization potential [13], porphyrins and related compounds have been central to studies of organic solar cells. In this review we will survey the various applications that have been reported to date and point out future directions that seem promising.

ORGANIC MOLECULAR SOLAR CELLS

Organic photovoltaic cells (OPVs) are an attractive approach to developing solar energy conversion devices due to the simple and inexpensive techniques needed for processing the photoactive layer. Spin casting, doctor blading, and inkjet printing of thin organic films have already led to solar cell device efficiencies around 5% for large area cells [14]. Porphyrins and phthalocyanines have played an important role in the understanding and the development of these types of photovoltaic devices. Since Tang's first report in 1986 of a heterojunction bilayer organic solar cell composed of Cu-phthalocyanine and a perylene derivative [15], the field has expanded rapidly and now includes a wide variety of "small" molecule solar cells containing phthalocyanines or porphyrins as dyes, conjugated polymers such as poly[2-methoxy-5-(3′,7′-dimethyloctyloxy)-1,4-phenylenevinylene] (MDMO-PPV) or poly(3-hexylthiophene) (P3HT) as the p-type donor phase, and C_{60} or perylene derivatives as the acceptor phase [16]. Cells are typically constructed using a transparent conductive glass like ITO (tin-doped indium oxide), followed by the deposition of a hole-injection layer such as poly(3,4-ethylenedioxythiophene) poly(styrenesulfonate) (PEDOT:PSS) that serves to make efficient electrical contact to the organic photoactive layer. The PEDOT:PSS also serves to smooth out the crystalline underlying ITO layer which, because of the extremely thin active layers (10–200 nm), can often serve as a contact point for a short-circuit in a solar cell device. The photoactive layers are evaporated, printed, or solution cast onto the ITO/PEDOT:PSS electrode.

As described earlier, the central photophysical processes observed in these types of devices are exciton generation in the light-absorbing (donor and/or acceptor) phase, exciton diffusion to the interface between donor and acceptor, exciton dissociation at the interface, and free charge carrier migration and collection at opposite electrodes. This mechanism is ascribed to both small molecule solar cells composed of phthalocyanines or porphyrins as well as polymer solar cells. The common acceptor in these cells is either C_{60} or the more soluble fullerene derivative [6,6]-phenyl-C_{61}-butyric acid methyl ester (PCBM), which is preferred for use in most BHJ solar cell configurations. A major goal in the field has been to understand all of these processes and to engineer cells that take advantage of molecular structures that optimize these photophysical processes [16–19]. In many cases, specific intermolecular interactions between donor and acceptor phases are also engineered to facilitate any or all of these critical processes. A large variety of porphyrin and phthalocyanine substrates have been evaluated both in single molecule form, and more recently, incorporated into macromolecular structures utilizing support polymers or directly integrated into a main chain polymer. In addition to molecular strategies evaluated, nanoscale phase engineering is currently being pursued in order to optimize the porphyrin donor and/or C_{60} acceptor morphologies that will allow for efficient exciton charge separation at all heterojunction interfaces. An overview of device configurations and assembly methods is presented that highlights porphyrin and phthalocyanine-based organic solar cell devices.

Evaporated thin films - phthalocyanine:C_{60} solar cells

A basic approach modeled after the original Tang cell assembles a bilayer heterojunction by sequential evaporation of both donor and acceptor materials onto a transparent conductive oxide surface such as ITO (Fig. 5). The cell is completed by evaporation of a back metal contact (typically with a work function more positive than ITO, *e.g.*, Al, Ca, Ag) and the performance assessed by illuminating through the glass electrode while measuring photocurrent/voltage response.

Crucial to the successful operation of such devices is the creation of an active layer with close interfacial contact between donor and acceptor phases for efficient exciton dissociation and successful collecting of free-charge carriers (electron and holes), while also being thick enough to harvest sunlight effectively. The light harvesting efficiency of this type of solar cell is dependent on active layer thickness and the absorption characteristics of the donor and acceptor materials. The charge separation and collection efficiency depends upon the

Copyright © 2010 World Scientific Publishing Company

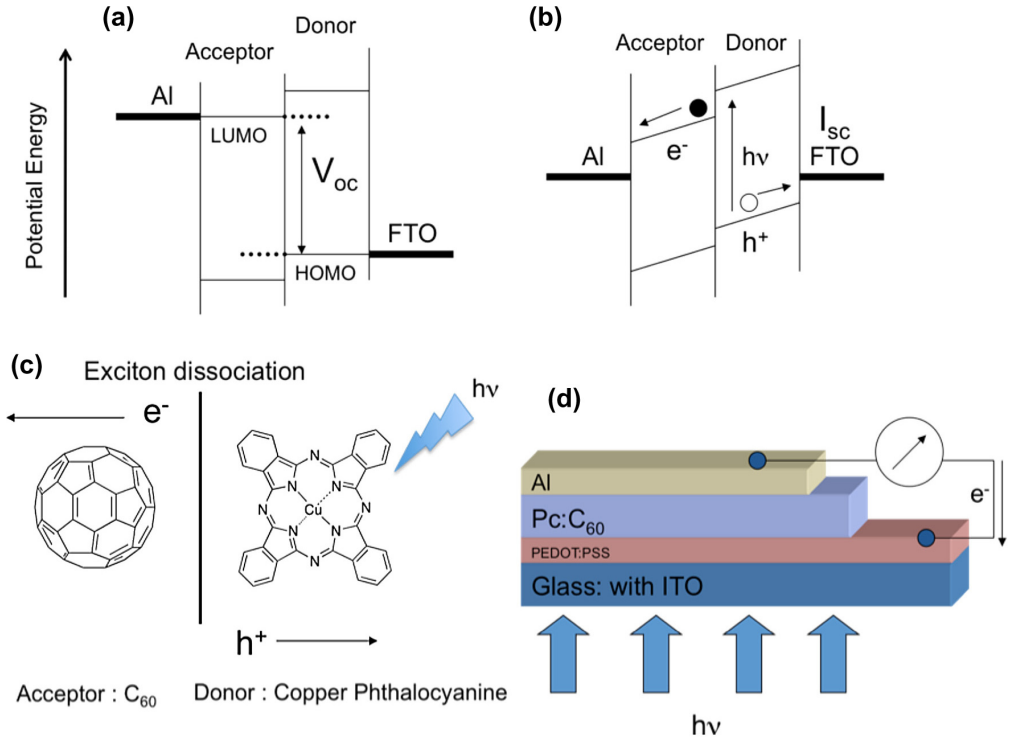

Fig. 5. (a) Open-circuit voltage (V_{oc}) condition for molecular solar cell. (b) Short-circuit conditions where an exciton dissociates at the interface (c) with free charge carriers moving through the donor phase (holes) and acceptor phase (electrons) to back contacts. (d) Solar cell configuration with active layer (phthalocyanine:C_{60}) deposited by evaporation onto an ITO-conductive glass electrode previously coated with a conductive polymer (PEDOT:PSS)

nanostructured environment relative to exciton diffusion lengths and charge mobilities of holes in the p-type donor layer and electrons in the n-type acceptor layer. The photovoltage is limited by the energy levels of the HOMO of the donor and the LUMO of the acceptor (Fig. 5a) [20]. The efficiency of charge separation is also related to the energy level differences between the corresponding HOMO and LUMO orbitals of the donor and the acceptor. For most organic polymers and molecular structures the energy required to separate an exciton into a hole and an electron must be larger than the Coulombic attraction between hole and electron, typically around 0.3–0.4 eV [21]. Assuming that all photogenerated free-charge carriers can be collected for a certain active layer thickness, the magnitude of the maximum photocurrent can be estimated by using the bandgap of the relevant absorber and integrating against the solar spectrum to that point – the conventional Shockley-Queisser limit for solar energy conversion [22].

Typically, the p-type donor phase is the primary absorber, but the n-type acceptor phase can also account for observed photocurrent. An exciton generated in either the donor or acceptor phases can move to an interface and dissociate into a hole and electron, provided the interface is located within the exciton diffusion length (L_{exc}) for that particular material. Exciton diffusion lengths are highly dependent on the nature and molecular orientation (crystallinity) of the material within the photoactive layer. For example, a self-assembled *meso*-tetrakis[3,5-bis(methoxymethyl)phenyl]porphyrinato zinc(II) thin film was found to have an exciton diffusion length of 15 nm based upon time-resolved microwave conductivity [23]. Typically phthalocyanine materials have much higher L_{exc} values due to their highly planar molecular structure that packs more closely, resulting in an increased crystallinity and thereby allowing for much stronger intermolecular electronic interactions. A diffusion length of 68 nm was determined for a CuPc using the measured photocurrent spectra and systematically varying layer thicknesses [24]. Band tilting (Fig. 5b) within the solar cell device is a result of differences in work function of the contact electrodes across a very thin insulating layer. While band tilting based on selective electrode contacts helps drive free charge carriers to be collected at either contact, it is not the limiting variable when determining the attainable open-circuit voltage (V_{oc}) for a given device.

Improving the overall efficiencies of these devices requires the tuning of the HOMO-LUMO gap of the phthalocyanine or porphyrin donor phase to increase the spectral response while maintaining a sufficiently energetic offset between the donor and acceptor to allow for efficient electron transfer. In addition, engineering the cell to allow for high hole and electron mobility requires molecular control and nanostructure control of both phases [25]. The mobility of free charge carriers is also highly dependant on the impurity concentration within the materials and can be adjusted by purposely adding dopants in the form of covalently attached ionic

Copyright © 2010 World Scientific Publishing Company

substituents [26] or by simply using lower purity materials [27].

Among the many molecular solar cell material configurations which have been examined, the phthalocyanine:C_{60} blend typically deposited by evaporating both phases onto an ITO electrode has been one of the most commonly pursued, with a wide range of efficiencies reported. The primary advantages of using phthalocyanines over porphyrins in a blended OPV are wider spectral range, longer exciton diffusion lengths, and higher hole mobility.

In 2001, Peumans and Forrest reported a highly efficient double-heterostructure copper phthalocyanine:C_{60} cell that incorporated an exciton-blocking layer with overall power conversion efficiency of 3.6% under 150 mW.cm^{-2} of illumination [28]. The cell used a photoactive phthalocyanine:C_{60} layer with a 0.4 nm thick bathocuproine (BCP) layer deposited on top to transport electrons while blocking excitons in the phthalocyanine layer from recombining at the anode. The device performed with J_{sc} = 18.8 mA.cm^{-2}, V_{oc} = 0.58 V and *ff* = 0.52 (Fig. 6a). Later work by Xue from the Forrest group demonstrated an increase in the efficiency of a CuPc:C_{60} solar cell (from η = 3.7% to η = 5.0%) by first evaporating a CuPc-only layer, followed by a co-evaporated 1:1 blend, and finally a homogeneous C_{60}-only layer [29]. The increase in efficiency was attributed to more efficient free-charge carrier collection provided for by the homogeneous layers of CuPc (holes) and C_{60} (electrons).

Increasing the solar spectral response of the photoactive layer is an important goal for organic solar cells, especially when utilizing porphyrins and phthalocyanines whose visible light absorbance onset is usually around 650 nm for porphyrins and around 750 nm for metallophthalocyanines (Cu, Zn, Pd). Dai *et al.* used a Pb-phthalocyanine to increase the spectral response into the near-IR for ZnPc:C_{60} cells resulting in photoconversion efficiencies of 1.95% [30]. It is unclear from this work what quantum yields were obtained in the longer wavelength regions (800–1000 nm), however, device efficiencies exceeded those using ZnPc:C_{60} only cells. Yang *et al.* demonstrated a blend of CuPc and SnPc to increase near-IR sensitivity, resulting in a device with 2.9% efficiency for a single heterogeneous photoactive layer device [31]. Both PbPc and SnPc structures have a less planar geometry, resulting in absorbance in the red and near-IR regions.

Other attempts at increasing the spectral response in the red and near-IR include work by Bailey-Salzman

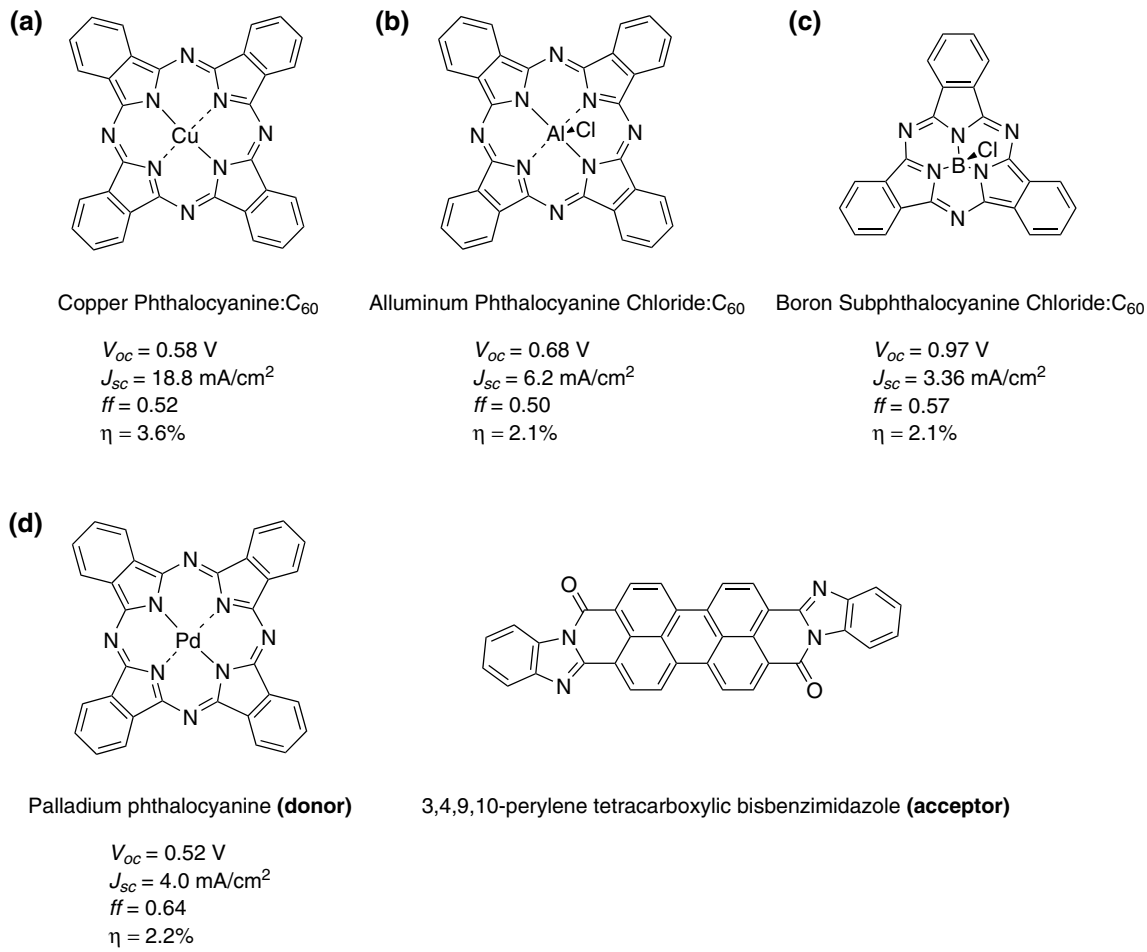

Fig. 6. Phthalocyanine/fullerene solar cells and their V_{oc}, J_{sc}, *ff*, and solar energy conversion efficiencies under AM1.5G, 100 mW.cm^{-2}. References: **(a)** [28] **(b)** [32] **(c)** [35] **(d)** [37]

Copyright © 2010 World Scientific Publishing Company

using a ClAlPc that also extends the spectral sensitivity into the near-IR (Fig. 6b) [32]. The report determined that nonplanar ClAlPc with a chloride axial ligand disrupts crystal packing in the Pc:C_{60} blend, resulting in an amorphous active layer. The devices exhibited solar conversion efficiencies of $\eta = 2.1\%$; although there was little increase in J_{sc} compared to the CuPc devices, a larger V_{oc} was obtained due to the lower energy level of the HOMO level of the ClAlPc derivative. Phthalocyanines containing TiO also exhibit a nonplanar structure and extended spectral response in the red/near-IR. Brumbach *et al.* reported a TiOPc:C_{60} solar cell and found that TiOPc:C_{60} had a larger HOMO/LUMO energy gap offset between the acceptor and donor phase than most Pc:C_{60} cells (1.1 eV compared with 0.7 eV for CuPc:C_{60}) [33]. The observed photovoltages for TiOPc:C_{60} were greater. However, it was found that there was also a lowering of the driving force for exciton dissociation, so that overall solar cell conversion properties were only slightly improved over CuPc:C_{60} devices ($\eta = 1.0$–1.4%).

A novel attempt by Varotto *et al.* to expand the spectral response in a Pc:C_{60} cell was accomplished by blending various thioalkane-substituted Pc chromophores containing band gaps varying from about 1.6 to 1.85 eV [34]. Solution-cast cells using blends of three different Pc dyes exhibited an increase in device performance from $\eta = 0.026\%$, 0.012%, and 0.033% for cells containing single chromophores to $\eta = 0.12\%$ for devices with a blend of all three Pc derivatives. The blended cell exhibited an increased J_{sc} of 1.24 mA.cm^{-2} and a V_{oc} of 0.408 V, representing a 0.1 V improvement over the highest performing single chromophore cell, with each Pc derivative contributing to the overall photocurrent as determined from IPCE measurements.

Work by Mutolo *et al.* demonstrated significant improvement in the open-circuit voltage of a Pc:C_{60} cell with the use of a strongly absorbing subphthalocyanine derivative (Fig. 6c) which increased V_{oc} from 0.42 V for a Cu-Pc:C_{60} device to 0.97 V for a B-SubPc:C_{60} device [35]. The larger observed V_{oc} agrees well with the observed lower HOMO level for subPc (0.69 V *vs*. Fc/Fc$^+$ reference) compared to Cu-Pc (0.29 V), *i.e.*, the energy gap between the HOMO of the donor to the LUMO of the acceptor was increased by 400 meV. A more efficient device (2.1%) was observed albeit with a slightly lowered fill factor and photocurrent.

Open-circuit voltages of up to 0.9 V were obtained with simple CuPc:Al Schottky contact solar cells. However, these devices suffer from low photocurrents as a result of high recombination in the CuPc layer [36]. The extraction of free charge carriers is limited by the thickness of the active layer, *i.e.*, a thicker layer is required for significant light absorption but limits the number of excitons that can diffuse to the metal/organic layer interface before recombining.

A wide variety of metallophthalocyanines have also been recently re-evaluated using both C_{60} and 3,4,9,10-perylene tetracarboxylic bisbenzimidazole (PTCBI) as an n-type acceptor layer. Kim *et al.* reported a 2.2% efficient PdPc evaporated thin film solar cell using PTCBI as the electron acceptor (Fig. 6d) [37]. The use of heavier atoms was proposed as a possible strategy to increase carrier mobility within the Pc donor layers.

A major challenge for the development of organic solar cells for commercial use is maintaining oxidative stability of evaporated thin films of organic materials for long periods of operation [38]. The primary degradation mechanism for conjugated polymer:fullerene solar cells is believed to be oxidation of the donor material. A proposed oxidative degradation mechanism involves the generation of singlet O_2 as a result of the long-lived triplet state of C_{60} molecules. Generated singlet O_2 is believed to be a possible contributor to the photodegradation of the p-type donor layers in various polymer and small molecule solar cells [39]. Therefore, when engineering organic solar cells and modules, encapsulation technologies will be important considerations when designing commercial cells for future applications. Studies have begun to determine the stability that can be imparted when sealing polymer solar cells using epoxy resins [40].

Tandem cells

Efforts have been made to increase the efficiencies of small molecule solar cells by using a tandem cell configuration, which offers the potential to increase the photovoltage as well as the spectral sensitivity to visible light [41]. Typically, this requires the construction of a stacked device structure with ohmic contacts between two subcells. The limitations of using organic polymer solar cells include a limited optical absorption of the donor layer, most commonly poly(3-hexylthiophene), P3HT. Therefore, several attempts have been made to increase the spectral response by layering a Pc:C_{60} photoactive layer on top of a P3HT:PCBM bulk-heterojunction polymer cell. Due to the series electrical configuration of the two subcells, photocurrent generation is limited to the lower of the two photocurrent densities generated, but photovoltages are potentially additive. A listing of several notable tandem organic solar cells is presented in Table 1, with both subcell and tandem cell solar conversion efficiencies.

An early report of a tandem configuration by Dennler *et al.* shows that the photovoltages obtained were approximately 1.6 times larger than the subcells alone [42]. They reported a ZnPc:C_{60}/P3HT:PCBM tandem cell that exhibited V_{oc} of 1.02 V with a J_{sc} of 4.8 mA.cm^{-2}, ff = 0.45, and $\eta = 2.3\%$. A thin, 10 nm gold film was used to ohmically connect both cells with the complementary absorbing materials stacked so that shorter wavelengths are absorbed in the P3HT:PCBM layer first, followed by longer wavelengths in the ZnPc:C_{60} layer.

Janssen *et al.* reported an organic tandem solar cell using a P3HT:PCBM blend as a base layer, followed by

Copyright © 2010 World Scientific Publishing Company

Table 1. Organic tandem solar cells (efficiencies of subcells reported when available). Irradiations at AM1.5G (100 mW/cm^2) except where noted

Active layer 1, η	Active layer 2, η	Cell details	V_{oc}, V	J_{sc}, mA/cm^2	*ff*	η, % [reference]
ZnPc:C_{60} (2.2%)	P3HT:PCBM (2.6%)	Au (10 nm) ohmic contact	1.02	4.8	0.45	2.3 [42]
CuPc:C_{60} (1.6%)	P3HT:PCBM (1.5%)	WO_3 (3 nm) interlayer	0.6	15.4 (160 mW/cm^2)	0.5	3.0 [43]
CuPc:C_{60} (2.19%)	PCPDTBT:PCBM (0.93%)	Ca/Al/MoO_3 (15 nm) interlayer	1.27	1.72	0.51	1.27 [45]
CuPc:C_{60}	CuPc:C_{60}	Ag (5 nm) nanoclusters	1.03	9.7	0.59	5.7 [46]
MeO-TPD/ZnPc:C_{60} (1.9%)	MeO-TPD/ZnPc:C_{60} (1.9%)	p-i-n tandem cell	0.85	6.6	0.53	2.4 [47]

the evaporation of a CuPc:C_{60} thin film on top of a 3 nm WO_3 contact interlayer to ohmically connect both cells [43]. The subcells separately exhibited solar conversion efficiencies of 1.5% for the P3HT:PCBM blend and 1.6% for the CuPc:C_{60} cell. The tandem cell exhibited efficiencies of 4.6% at low light intensities (16 mW.cm^{-2}). This was a significant increase in the conversion efficiencies of previous tandem cell reports (η = 1.2, 2.3%) [42, 44] where the efficiency of the tandem was lower than that of the individual subcells. This was also observed in a recent report by Zhao *et al.* in which the V_{oc} values increased with the tandem configuration using poly[2,7-(9,9-dihexylfluorene)-alt-bithiophene and PCBM (V_{oc} = 1.27 V) [45]. However, a significant loss in photocurrent density (single cell J_{sc} = 4.27 mA.cm^{-2}, tandem cell = 1.75 mA.cm^{-2}) limited the overall conversion efficiency to 1.27% when combined in a tandem configuration with CuPc:C_{60} as the top cell.

The highest efficiency for a tandem device structure was reported by Xue *et al.* who reported a tandem cell using two CuPc:C_{60} subcells stacked in series [46]. The cell operated with J_{sc} = 9.7 mA.cm^{-2}, V_{oc} = 1.03, *ff* = 0.59 and η = 5.7%. The ohmic connection between both cells was made with a 5 nm thick Ag nanocluster layer where majority carriers can recombine. Maennig *et al.* developed a unique organic p-i-n solar cell whereby an intrinsic undoped region is sandwiched between a p-doped active layer and an n-doped wide-gap layer [47]. The photoactive layer was a mixture of ZnPc:C_{60} and exhibited external quantum efficiencies of 40% between 630 and 700 nm. A power conversion efficiency of 1.9% was obtained for a single cell and 2.4% was obtained for the tandem device using two p-i-n layers: p-type MeO-TPD/ZnPc:C_{60}/and an n-doped C_{60}.

Solution-cast donor/acceptor thin films

Takahashi *et al.* have demonstrated some of the highest efficiency spin-cast thin film solar cells in which a porphyrin is incorporated as the primary photoactive material. The work includes the use of metallated and free-base porphyrin structures deposited on Al-coated glass electrodes with photoactive layer thicknesses of 30–40 nm. A Zn tetraphenylporphyrin and Rhodamine B-blended thin film was first demonstrated to show photovoltaic properties when configured in the Schottky cell Al/dye/Au device structure with ϕ = 14.7% at 440 nm monochromatic light with V_{oc} = 0.9, *ff* = 0.18 and monochromatic energy conversion efficiency of 0.82% [48]. Further investigations using blends of donor (tetra(2,5-dimethoxyphenyl) porphyrin) and a metal-free acceptor (5,10-diphenyl-15, 20-bis(3-pyridyl)porphyrin yielded solar cells with a monochromatic energy conversion efficiency (445 nm) of 1.5% (Fig. 7a) [49]. Increased photocurrents were observed with a blend compared to either single porphyrin, which was attributed to the formation of a heterodimer complex with the pyridyl substituent of the acceptor binding to the central Zn atom on the dimethoxyphenyl-containing donor porphyrin. The cells had active layers of 19 nm and exhibited ϕ = 18.9% at 445 nm, V_{oc} = 0.79 V, *ff* = 0.23, and η = 1.2%. Interestingly, the addition of P3HT in this device geometry to serve as a hole conductor slightly lowered the overall efficiencies (η = 1.0%); however, the presence of the porphyrins greatly increased the photocurrent over devices using only P3HT [50].

Thin porphyrin or phthalocyanine films with electron acceptor C_{60} or PCBM

It has been demonstrated that there exists a high binding affinity between the tetraphenylporphyrin macrocycle and C_{60} structures, leading to efficient quenching of porphyrin fluorescence by fullerene moieties in either self-assembled or dyad-linked structures [51–53]. Structures utilizing porphyrin/C_{60} nanoclusters and self-assembled monolayers organized on ITO arrays have been reported to give good quantum efficiencies up to 17% for extremely thin layered devices (~5 nm) [54, 55]. While overall solar power conversion efficiencies are modest, the photoinduced electron transfer occurring between porphyrin and fullerene is a highly efficient process which will require further nanostructure development and/or interfacial engineering to efficiently extract photogenerated free-charge carriers.

To both improve processability of a Pc:PCBM blend and to extend the spectral absorbance window into the

Copyright © 2010 World Scientific Publishing Company

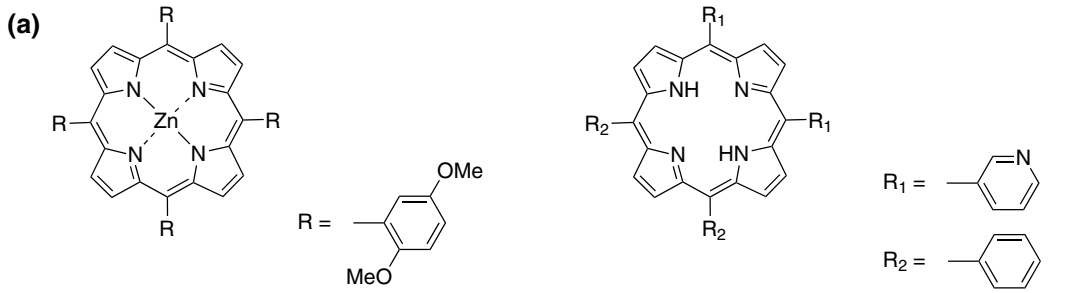

Zinc tetrakis(2,5-dimethoxyphenyl)porphyrin **(donor)**

5,10-diphenyl-15,20-bis(3-pyridyl)porphyrin **(acceptor)**

V_{oc} = 0.89 V
J_{sc} = 0.015 mA/cm^2 (20 mW.cm^{-2}) 445 nm
ff = 0.21
η = 1.5%

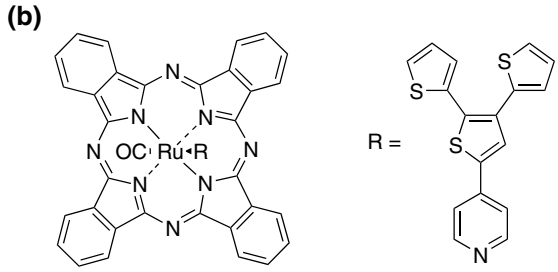

Ruthenium PcCOPy-nT:PCBM

V_{oc} = 0.56 V
J_{sc} = 8.3 mA/cm^2
ff = 0.34
η = 1.6%

Fig. 7. Photovoltaic performance of porphyrin/phthalocyanines used in thin-film solution-cast solar cells. References: **(a)** [49] **(b)** [56]

380–550 nm range, a novel ruthenium(II) phthalocyanine (RuPc) complex with a dendritic oligothiophene ligand in the axial positions was synthesized and tested in a blended PCBM bulk heterojunction solar cell with an active layer around 60–90 nm thick (Fig. 7b) [56]. The blend with a 1:2 ratio of donor:acceptor was spin-cast onto PEDOT:PSS-coated ITO substrates. The increased absorption window resulted in efficiencies up to 1.6% which, to date, is the most efficient reported blended Pc:PCBM organic solar cell. The electrochemical properties of these Pc complexes indicated sufficiently large LUMO donor – LUMO acceptor energy differences to allow for exciton dissociation and efficient electron transfer from the RuPc complex to the PCBM acceptor at their interfaces.

A recent Zn porphyrin:fullerene blend reported by Oku *et al.* used a derivatized perylene as an exciton-blocking layer, increasing photocurrent densities from 0.074 mA.cm^{-2} to 0.62 mA.cm^{-2} [57]. Although the overall solar conversion efficiencies of these devices were low (η = 0.08%), the advantage of the cell was the simplicity of the device construction using spin casting thin films of the photoactive layer (ZnTPP:C_{60} blends) directly onto PEDOT:PSS coated ITO substrates. In this configuration, a thin film of 3,4,9,10-perylenetetracarboxylic dianhydride was solution-cast directly on top of the photoactive ZnTPP:C_{60} layer in order to prevent hole transfer to the Al contact anode.

Self-assembled films (liquid crystal) solar cells

Novel liquid crystal porphyrins, *e.g.*, zinc octakis-β-decoxyethylporphyrin (ZnODEP), have allowed the simple processing technique of melt casting between two conductive ITO glass electrodes. These systems were used to demonstrate the effects of charging a thin, polycrystalline, photoactive film, where the charge can be maintained for a significantly long time, as a primitive memory device [58]. A similar liquid crystal porphyrin (zinc octakis-β-nonoxyethylporphyrin) was found to have high hole mobility due to its highly regular packing within the polycrystalline films [59]. Mobilities as high

Copyright © 2010 World Scientific Publishing Company

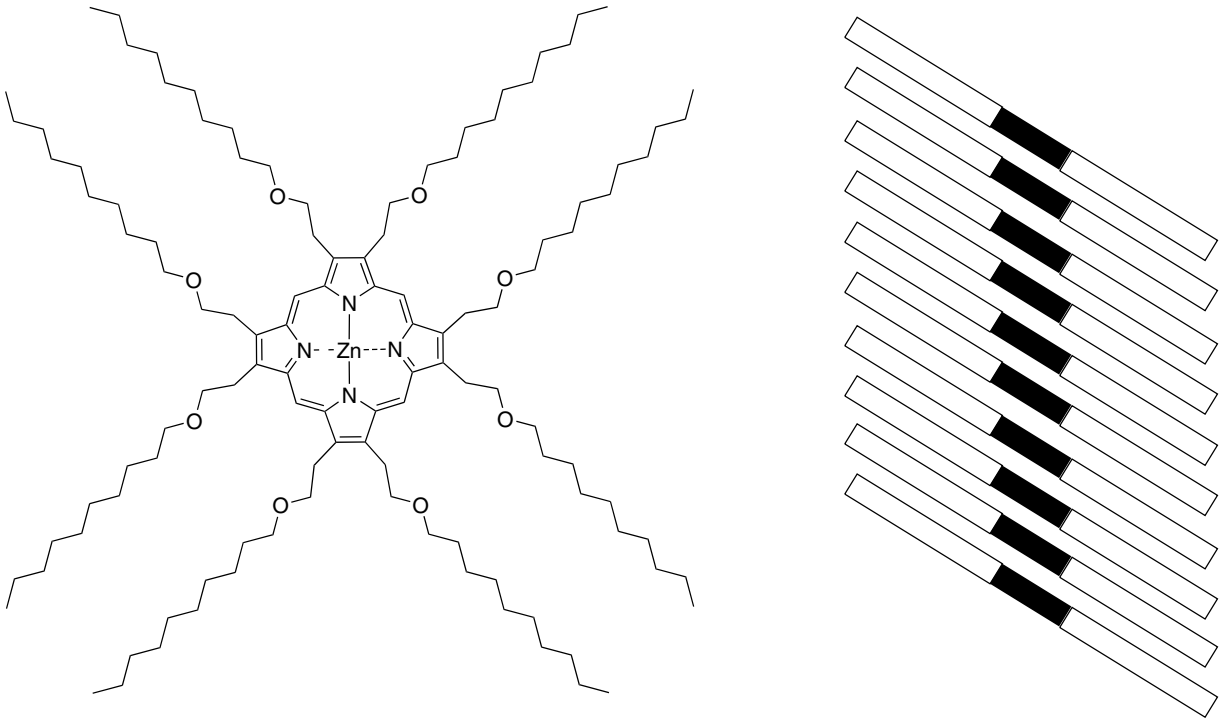

Fig. 8. Zinc octakis-β-decoxyethylporphyrin (ZnODEP), which orients in liquid crystalline films [58–61]

as $\mu_h = 2.6 \times 10^{-6}$ m^2.V^{-1}.s^{-1} were observed, and X-ray data indicated a tilted molecular orientation with respect to the plane of the electrodes (Fig. 8). Charge carriers move efficiently through the porphyrin units, which are electronically insulated by the long alkyl chains. These types of systems were evaluated as a solar cell configuration using (zinc octakis-β-octyloxyethyl)porphyrin melt cast between two ITO electrodes using spacers with 0.8–8.0 μm thickness [60]. Interestingly, because the device configuration used identical ITO electrodes, the photovoltage directionality depended on which side of the cell was being illuminated; the illuminated side became the negative photoanode. These devices exhibited high V_{oc} values (nearly 1 V) but modest photocurrents J_{sc} ~ 0.25 mA/cm^2 for a 1.5 μm thick device. A significant increase in the quantum efficiency (at 400 nm) of a ZnODEP device was later demonstrated by Liu and Bard by applying an electric field to the device (2000 V/cm). Quantum efficiency increased from 0.69% to 8.4%, ascribed to the effect of the electric field to trap space charges thereby encouraging free charge carrier movement through the device [61].

Recent work by Sun *et al.* and Kang *et al.* studying liquid crystal porphyrin structures and their incorporation into a bulk heterojunction solar cell have shown promising results for a recently developed LC porphyrin system (Fig. 9a) [11, 62]. The solar cell incorporated a 5,10,15,20-tetrakis[*p*-(3′,4′,5′-tris-pentadecoxybenzoyl) phenyl]porphyrin blended together with PCBM and deposited by spin coating the photoactive layer on a PEDOT:PSS-coated ITO electrode. The performance of the cell was greatly improved by applying both a bulk heterojunction strategy, as opposed to a bilayer configuration, and through thermal annealing of the blended photoactive layer. The device exhibited V_{oc} of 0.52 V and J_{sc} up to 5 mA/cm^2, resulting in a device with solar conversion efficiencies of 0.78%. The annealing step increased the device performance from 0.12% to 0.78%. Remarkably, it was shown later by the same group that the liquid crystal porphyrins and PCBM form a unique homeotropic alignment, with liquid crystalline porphyrin columns while maintaining a significant concentration of PCBM within the aligned liquid crystal phase [63]. They proposed a structure that includes a nanostructured alignment of porphyrins; this could represent an ideal configuration for a liquid crystalline organic solar cell if there were also a continuous phase of PCBM infiltrated between the columns of the donor porphyrin phase (Fig. 9a).

Another unique arrangement of porphyrins and C_{60} was recently reported by Sandanayaka *et al.* where a zinc *meso*-tetra(4-pyridyl)porphyrin was used to form hexagonal hollow nanotubes (2–7 mm long, 500–900 nm diameter) which were filled with C_{60} and C_{70} [64]. Quenching studies determined that the excited state of the self-assembled zinc porphyrin nanotube was quenched by the fullerenes, and that FTO electrodes modified with the C_{60} nanotubes exhibited an efficiency of $\eta = 0.63\%$ with $V_{oc} = 0.35$ V and $J_{sc} = 1.0$ mA.cm^{-2} in a regenerative I^-/I_3^- photoelectrochemical cell. The nanotube-only modified electrode exhibited an η of only 0.03%, which clearly demonstrated the importance of the C_{60} encapsulation within the porphyrin nanostructures (Fig. 9b).

Hasobe and co-workers developed an efficient porphyrin-fullerene solar cell using a porphyrin-alkanethiolate

Copyright © 2010 World Scientific Publishing Company

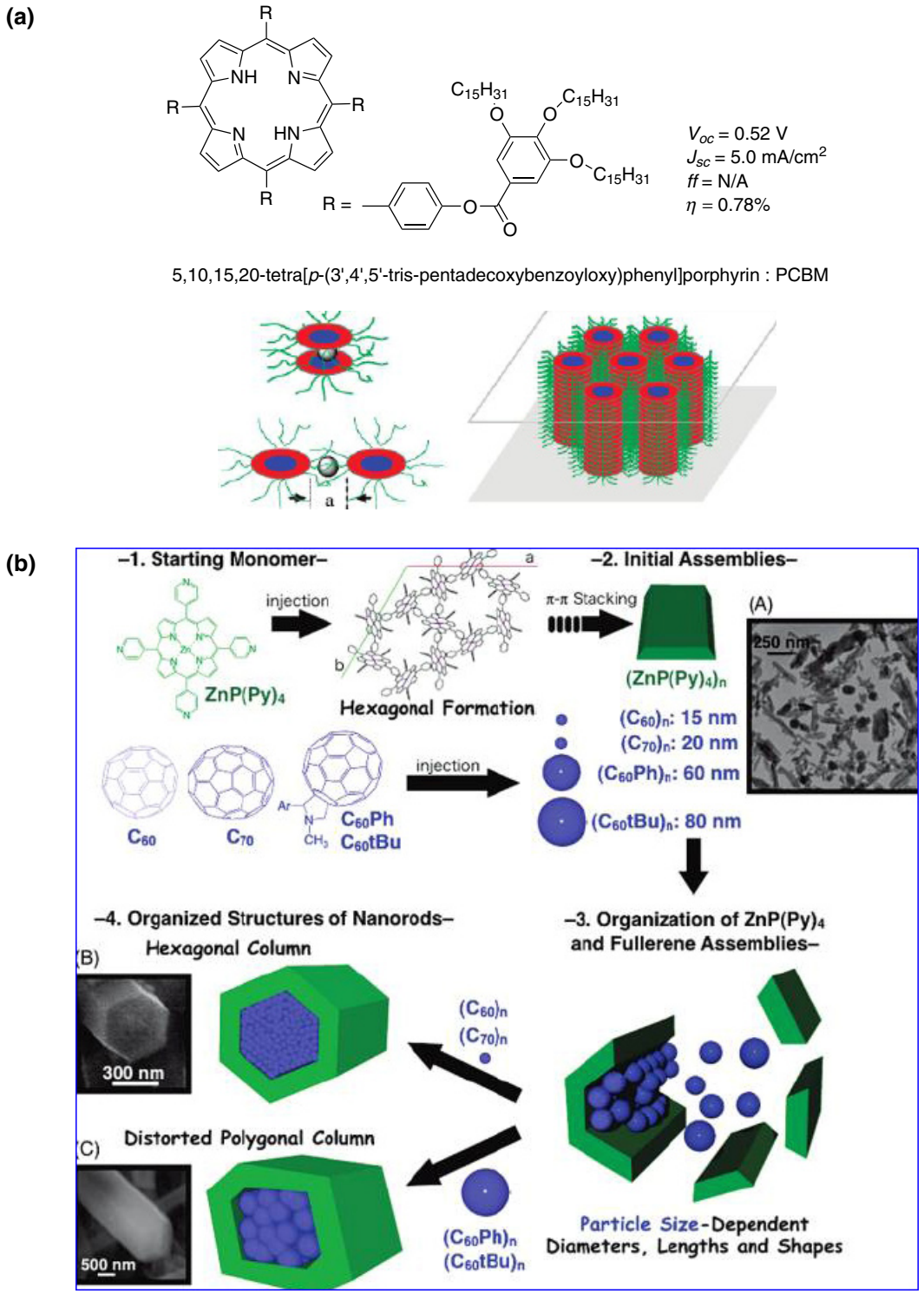

Fig. 9. (a) Liquid crystal porphyrin with PCBM between columns, structures and efficiencies [11, 62]. (b) C_{60}-filled Zn tetrapyridylporphyrin self-assembled nanorods [64]

monolayer-protected gold nanoparticle [65, 66]. The porphyrin-modified gold nanoparticles self-assemble with C_{60}, forming complexes that have C_{60} molecules inserted between pairs of porphyrin molecules attached to the gold nanoparticle (Fig. 10). Films of the clusters deposited on FTO exhibited ϕ = 45% (at 450 nm) and overall solar conversion η = 1.5% tested in a photoelectrochemical cell using (I^-/I_3^-) redox couple. The high photocurrent generation combined with the high quantum yield for this structure clearly suggests the importance of organizing supramolecular structures in such a way as to optimize the light-harvesting ability of the porphyrin dyes while controlling the morphology for efficient charge collection [67].

Copyright © 2010 World Scientific Publishing Company

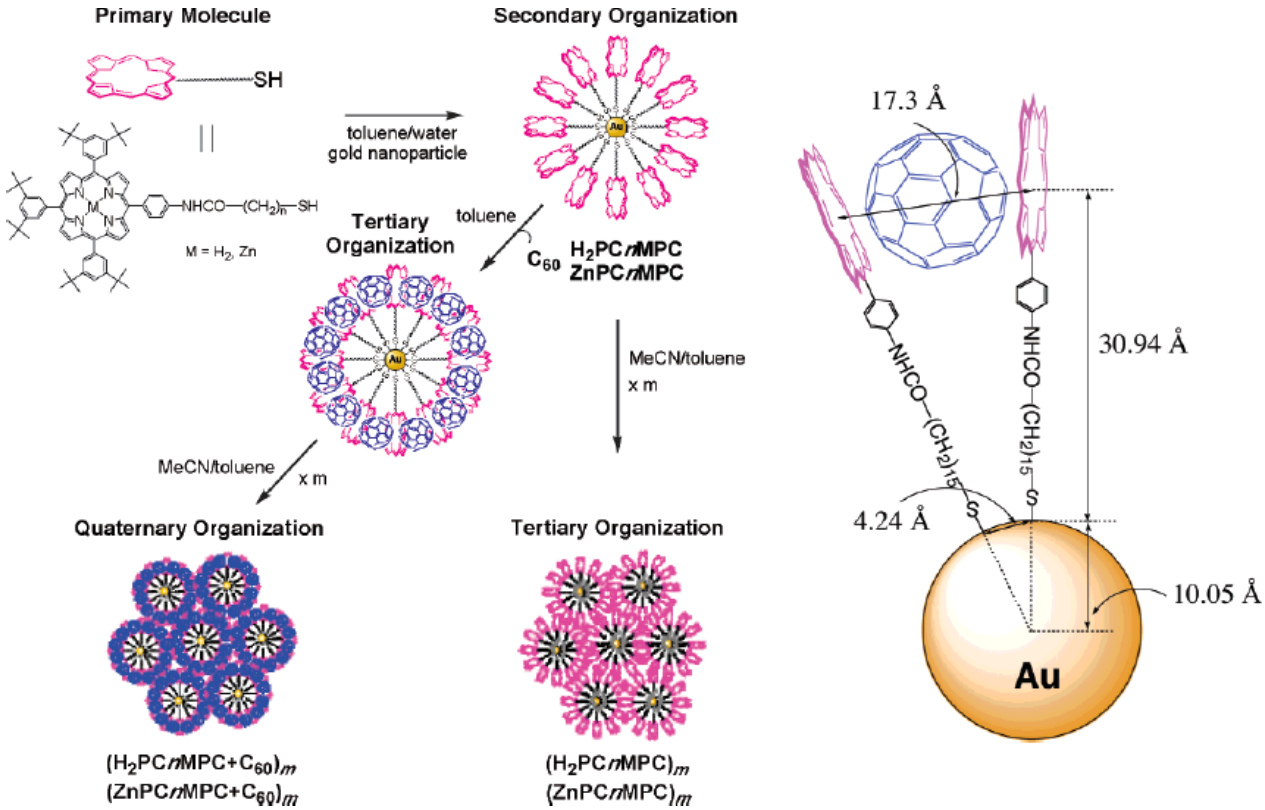

Fig. 10. Porphyrin-fullerene assembly on a Au nanoparticle. Solar cell performance: V_{oc} = 0.38 V, J_{sc} = 1.0 mA.cm^{-2}, *ff* = 0.43, η = 1.5% [65, 66]

Dyads, triads and oligomers

One strategy to increase the probability of photoinduced electron transfer between donor and acceptor layers within a molecular solar cell has involved the study of systems which have been covalently tethered together to encourage rapid photoinduced charge transfer. A large body of literature exists which examines the light-harvesting and energy transfer properties of porphyrin and phthalocyanine dyads, typically linked with C_{60} moieties or with the porphyrin and phthalocyanine derivatives linked directly together [55, 68–72]. In addition, several authors have examined systems designed to mimic the photosynthetic reaction center with supramolecular structures designed to utilize an energy cascade through structures assembled with porphyrin complexes [8, 73]. These systems have been examined using time-resolved photoinduced absorption measurements and luminescence quenching studies to evaluate rates of charge migration and the lifetimes of the various states [74]. For example, Escosura *et al.* reported that covalently linking a Zn phthalocyanine to a functionalized fullerene ultimately led to a significantly longer lifetime of the charge-separated state (475 ns) when an additional phthalocyanine was complexed to the Zn:Pc dyad [75]. A copper porphyrin-styrene-C_{60} dyad exhibited a similarly long charge-separation lifetime, with up to 415 ns observed for the CuP^{+}-C_{60}^{-} state [52]. Other similar porphyrin-C_{60} dyad systems showed charged separation lifetimes that were also sensitive to metal cation used in the porphyrin structure using the same dyad linked structure [76]. Significantly increased yields of charge-separated species in solution typically indicate a faster and more efficient charge separation, while significantly increased lifetimes of charge-separated species in solution are an indicator of decreased rates of charge recombination. Increased yields and lifetimes have been seen with a wide variety of porphyrin [8, 69, 77–79] and phthalocyanine dyads/triads [75, 80] with covalently attached electron acceptors such at C_{60}. Work reviewed here will examine those structures that have been incorporated into organic photovoltaic configurations.

Kaunisto *et al.* demonstrated interlayer electron transfer from a Zn phthalocyanine to a porphyrin fullerene dyad by studying the time-resolved photovoltages of the composite material [81, 82]. The mixtures of the porphyrin dyad and phthalocyanine exhibited maximum external quantum efficiencies of 0.8% (430 nm) with overall conversion efficiencies of about 0.024%. The same group reported the use of this dyad with an additional Zn porphyrin attached to an ITO electrode and reported quantum efficiencies as high as ϕ = 1.25% [55]. A dependence on the configuration of the Zn porphyrin connection to the ITO electrode and the porphyrin:C_{60} dyad resulted in higher efficiencies being observed for the *trans* configuration (Fig. 11), suggesting more efficient charge transfer for porphyrins with cofacial geometries.

Cells developed by attaching dyads and triads onto an ITO substrate and evaluated in an electrochemical cell or

Copyright © 2010 World Scientific Publishing Company

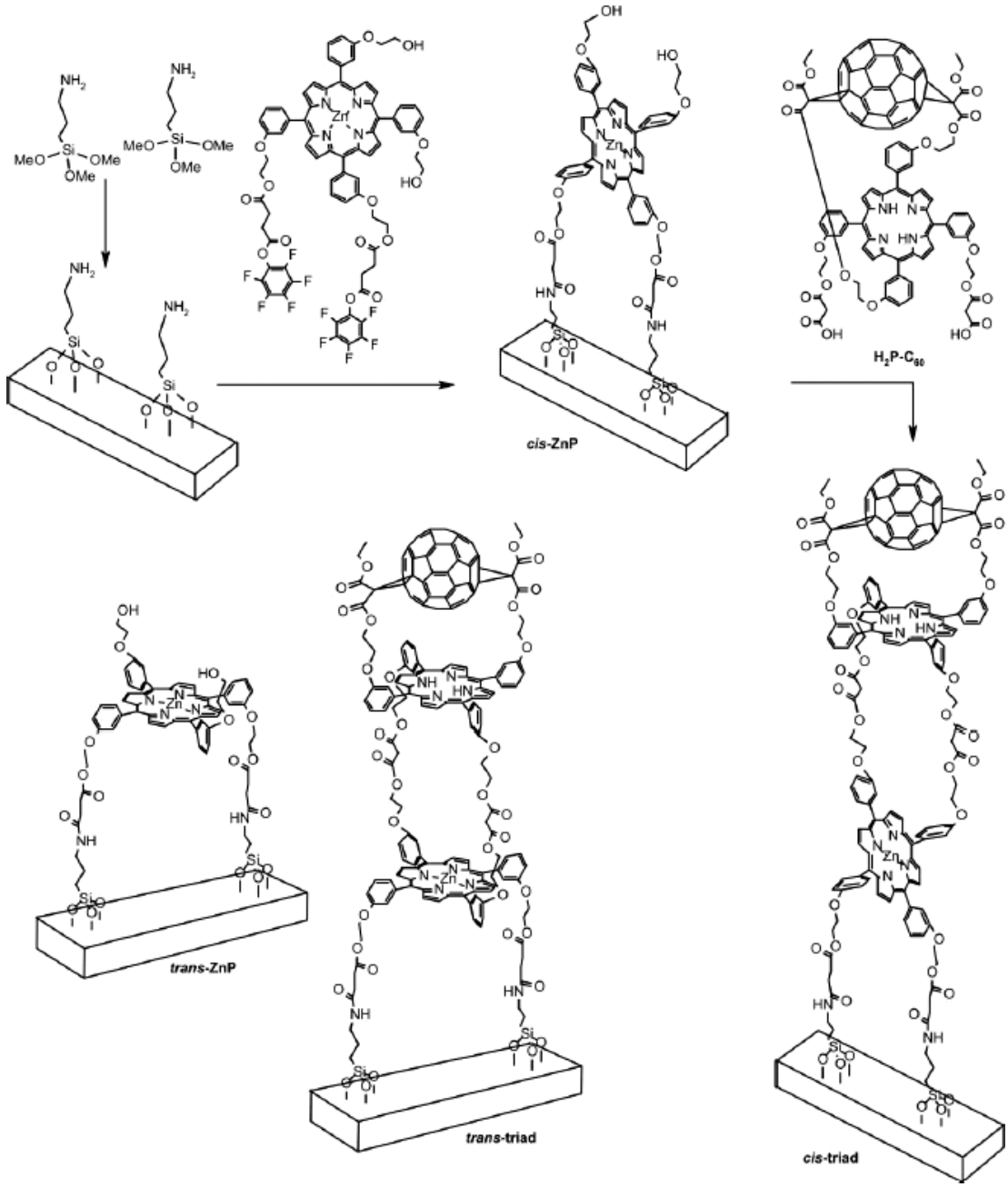

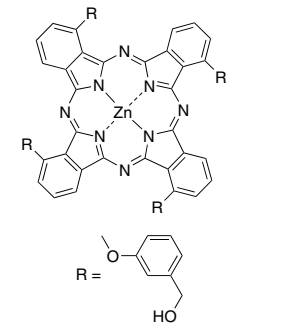

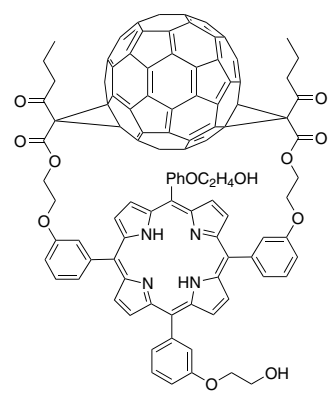

Zinc - phthalocyanine: porphyrin C_{60} dyad

V_{oc} = 0.2 V
J_{sc} = 1.29 mA/cm^2
ff = 0.2
η = 0.024%

Fig. 11. *Cis/trans* ZnP-C_{60} triad structures on ITO [55]

Copyright © 2010 World Scientific Publishing Company

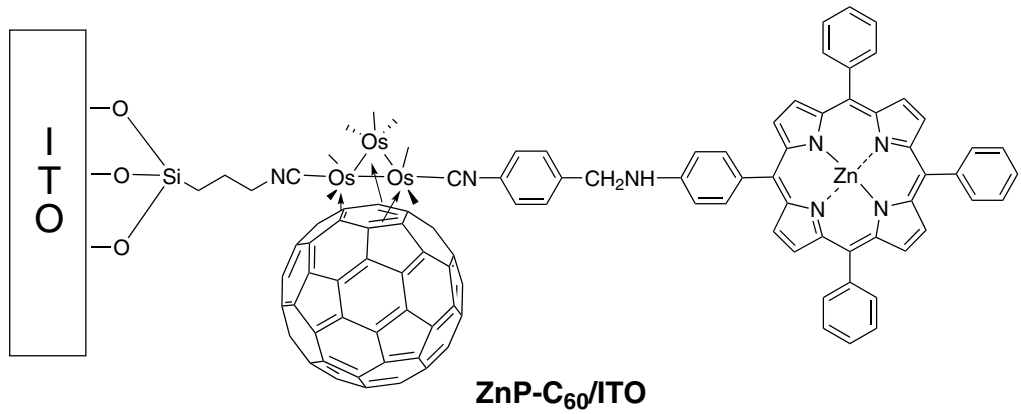

Fig. 12. ZnP-C_{60} dyad (Os) structure on ITO [70]

solid-state configuration demonstrate effective methods used to analyze these molecular configurations [70, 83]. Cho *et al.* developed a cell using a porphyrin-fullerene linked dyad that was attached to an ITO substrate using a 3-(triethoxysilyl)propyl isocyanide as a surface-anchoring ligand (Fig. 12) [70]. The cell was evaluated in an electrochemical configuration with ascorbic acid as a sacrificial electron donor and demonstrated ϕ of 19.5% (at 430 nm).

A bilayer Zn phthalocyanine:fullerene solar cell was incorporated with a pyrollidinofullerene compound with chelating pyridyl groups that complex with the Zn phthalocyanine (ZnPc) molecule [84]. A significantly increased solar cell performance was achieved when the ZnPc was used with the pyrollidinofullerene chelating compound as compared to the use of a PCBM acceptor layer; the observation was a doubling of J_{sc} from 2 to 4 mA.cm^{-2} with a solar conversion efficiency up to 0.5% (Fig. 13).

Hasobe *et al.* compared the photovoltaic properties of a ZnP-C_{60} dyad system with dendritic porphyrin structures containing up to sixteen porphyrin units per compound [85]. The porphyrin dendrimers were mixed with C_{60} and deposited electrophoretically onto nanostructured

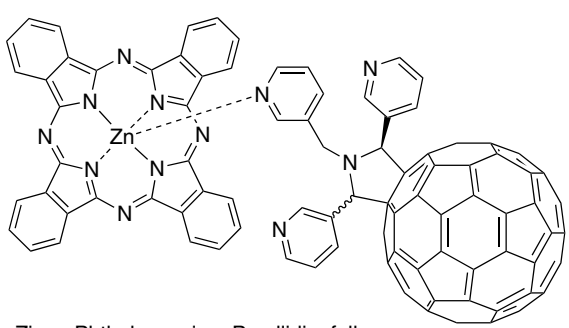

Zinc - Phthalocyanine: Pyrollidinofullerene

V_{oc} = 0.4 V
J_{sc} = 2.7 mA/cm^2
ff = 0.4
η = 0.5%

Fig. 13. ZnPc-C_{60} dyad solar cell and its photovoltaic properties [84]

SnO_2 films and then tested in a regenerative (I^-/I_3^-) electrochemical cell. The work found that the dendritic porphyrin:C_{60} composite film devices gave significantly higher values (J_{sc} = 0.29 mA.cm^{-2}, V_{oc} = 0.22 V, *ff* = 0.31) than the porphyrin:C_{60} dyad films. The supramolecular porphyrin clusters formed an interpenetrating network structure with C_{60} and provided a broader photoresponse in the visible and near-infrared regions.

ORGANIC POLYMER SOLAR CELLS

Porphyrins or phthalocyanines incorporated into polymer solar cells

Several authors have reported using porphyrin dyes blended directly with poly(3-hexylthiophene) (P3HT) [50]. For example, a simple solution processable device incorporating chlorophyll into P3HT has indicated promising light-to-current conversion efficiencies of 1.48% [86]. Devices like these take advantage of materials that are widely used and optimized for efficient thin-film organic solar cells such as polythiophene hole-conducting materials and electron-accepting fullerenes.

Dastoor *et al.* reported a solid-state porphyrin bulk heterojunction solar cell using a PCBM/MEH-PPV blend that performed with a 40% peak IPCE. Including a tetraphenylporphyrin derivative in the polymer/fullerene blend led to a broader absorption spectrum that improved the IPCE from 60 to 80% [87]. Burke reported the role of solvent trapping effects during processing and annealing in determining the morphology of a polymer solar cell when a Cu-2,3,12,13-tetracyano-5,10,15,20-tetrakis(3,5-di-*tert*-butylphenyl)porphyrin was blended with a P3HT:PCBM photoactive layer [88]. The presence of the porphyrin affected the nanoscale properties of the film with an increased disorder and bubble formation with increasing porphyrin concentration in the blend, specifically aggregation of porphyrins during the annealing step formed pockets that trapped solvent within the photoactive film.

Copyright © 2010 World Scientific Publishing Company

Main-chain porphyrin polymers

Porphyrins have been decorated with a variety of substituents that allow them to be polymerized either chemically or electrochemically. For example, Maree and Savenije analyzed the electrical properties of electropolymerized Zn and Pd-tetra(p-hydroxyphenyl)porphyrin polymers for use in a heterojunction solar cell composed of donor and acceptor porphyrin layers (Fig. 15a) [89, 90]. Using the electropolymerized porphyrin film deposited on ITO as the donor layer and a top acceptor layer composed of tetra(N-methylpyridinium)porphyrin, the devices demonstrate good V_{oc} values (0.4–0.6 V) but low J_{sc} values, likely due to limited electronic conductivity in these materials. The directionality of the photocurrent was verified to be related to a successful donor/acceptor heterojunction obtained with the spin-cast tetra(N-methylpyridinium)porphyrin cast directly on top of the electropolymerized film and was not a result of a Schottky contact between the organic layers and the evaporated Ag or bottom ITO contacts [91].

Akiyama *et al.* demonstrated an electropolymerized porphyrin-based device using a poly(tetrathienyl) porphyrin which was electrochemically deposited onto a previously electrochemically deposited bithiophene layer which had been deposited initially on top of a poly(3-dodecylthiophene) spin-cast base layer (Fig. 15b) [92]. The device was completed by evaporation of a Al top contact, creating a Schottky contact type cell. Photocurrents obtained for this type of device were low (13 $\mu A.cm^{-2}$ mW^{-1} at 440 nm). As described previously, strategies incorporating porphyrins into conjugated polythiophene hole-conductor layers have yielded much higher quantum efficiencies of $\phi \sim 18$–19% [50], making these types of strategies a more promising route to optimizing thiophene-containing porphyrin solar cells.

Preliminary work using a nanostructured tetra(aminophenyl)porphyrin film that was electrochemically deposited onto an ITO electrode with a solution-cast PCBM acceptor layer gave a bulk heterojunction solar cell with modest $V_{oc} \sim 0.3$ V and $J_{sc} \sim 0.2$ mA/cm^2 [12, 93]. The unique strategy of this work was focused on using the electropolymerized nanostructured polyporphyrin film to direct the interface between the porphyrin donor phase and the electron acceptor phase, the fullerene derivative PCBM. The high surface area of the nanofibers (40–100 nm diameter) of porphyrin polymer (Fig. 14) should, in principle, allow for short exciton diffusion to an interface between the porphyrin and fullerene for efficient exciton dissociation.

Copolymers

Several reports exemplify efforts to increase the light-harvesting properties of the p-type donor phase in a bulk heterojunction solar cell by incorporating strongly light-absorbing chromophores into the backbone of the conjugated polymer phase. The commonly used P3HT in the form of a slowly annealed spin-cast film provides significant solar harvesting with an absorbance onset of about 650 nm. To increase the overall light-harvesting ability of the polythiophene donor phase, several instances of tetraphenylporphyrins incorporated into the polymer backbone using either synthetic or electrochemical deposition techniques have been reported. These strategies have increased the light absorbance of the photoactive layer, however, solar conversion efficiencies have remained low due to the lowered hole mobility that incorporating porphyrin units imparts to the p-type donor phase.

In general, tetraphenylporphyrin films show low free charge carrier mobilities, limiting their use in various optoelectronic devices. Most conjugated organic materials such as P3HT and phthalocyanines exhibit hole mobilities (μ_h) on the order of ~15 $cm^2.V^{-1}.s^{-1}$ while thin porphyrin films have been observed to exhibit mobilities around 10^{-3} $cm^2.V^{-1}.s^{-1}$ [18, 59]. Lowered mobilities are associated with the large dihedral angle between porphyrin monomers that limit both the crystallinity of the

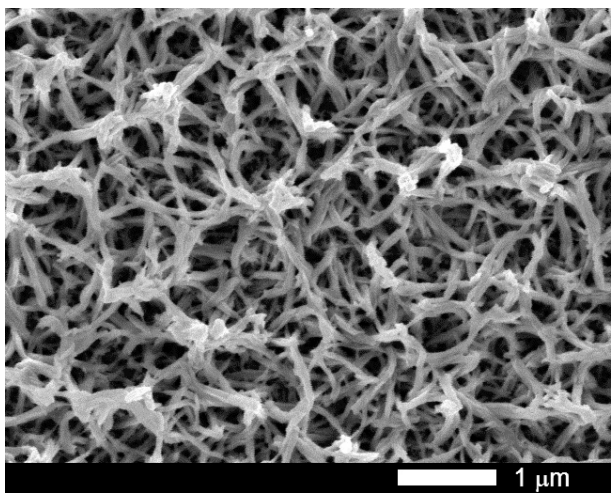

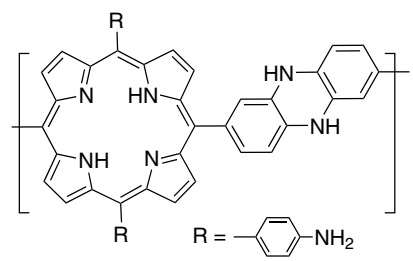

Poly(tetraaminophenylporphyrin):PCBM

V_{oc} = 0.30 V
J_{sc} = 0.18 mA/cm^2
ff = 0.29
η = 0.02%

Fig. 14. A nanostructured electropolymerized poly-TAPP film on FTO glass and photovoltaic properties with PCBM [12, 93]

Copyright © 2010 World Scientific Publishing Company

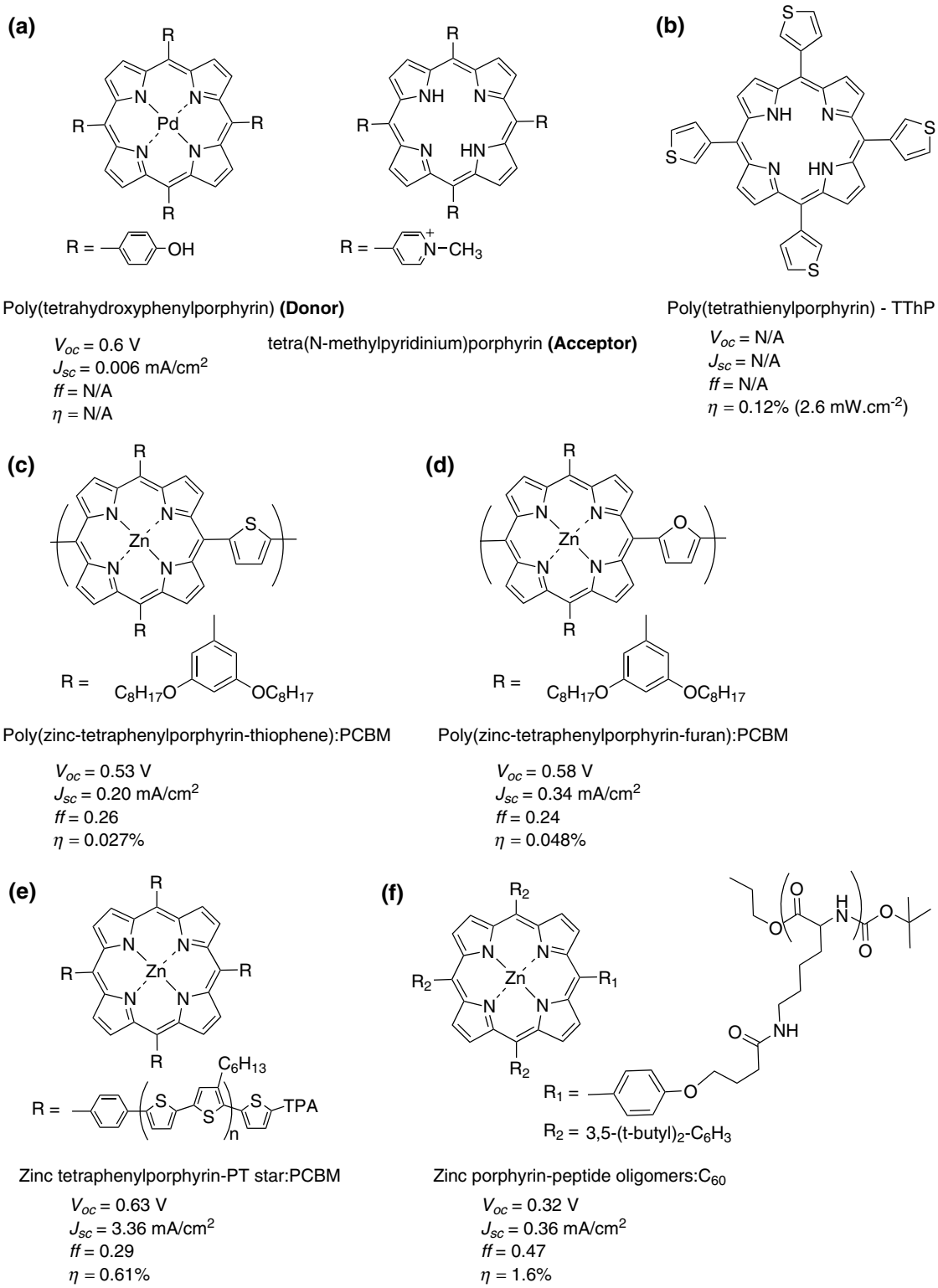

Fig. 15. Porphyrin polymer and copolymer structures with V_{oc}, J_{sc}, *ff*, and solar energy conversion efficiencies. References: (**a**) [89, 90] (**b**) [92] (**c,d**) [94] (**e**) [95] (**f**) [96]

obtained films and the extent of π-conjugation overlap within the polymer chains.

To test the effects of main-chain polymer incorporation, Umeyama *et al.* used palladium-catalyzed coupling reactions to synthesize novel conjugated copolymers of zinc porphyrin with both thiophene (Fig. 15c) and furan (Fig. 15d) moieties [94]. Blends of the copolymer with PCBM yielded solar energy conversion efficiencies of 0.048% for the furan-containing porphyrin polymer and 0.027% for the thiophene derivative. A slightly smaller

Copyright © 2010 World Scientific Publishing Company

bandgap was obtained with the furan-containing copolymer, with a red-shifted steady-state fluorescence spectrum compared with the thiophene derivative. A more extended π-conjugation along the polymer chain between porphyrin and furan units is believed to result from the smaller steric repulsion that a *meso*-substituted furan moiety has with the *beta*-pyrrole hydrogens. In these instances, incorporating the porphyrin moiety into the main chain of the polymer donor layer successfully increases the light-harvesting ability but sacrifices hole mobility.

Photovoltaic properties of polythiophene stars with zinc tetraphenylporphyrin (ZnTPP) core have been reported by Liu *et al.* (Fig. 15e) [95]. ZnTPP with four polythiophene chains showed modest efficiencies in BHJ cells with PCBM (0.6%) and was also used efficiently in a dye-sensitized solar cell with an efficiency of 3.9%. Polythiophene stars with porphyrin centers showed average molecular weights between 4000–7400 and exhibited increased absorption in the 450–650 nm region. The absorption spectra indicate that increasing the number of polythiophene units attached to the *meso*-positions of the porphyrin increased the absorbance beyond 550 nm and suppressed the photoluminescence of the porphyrin core.

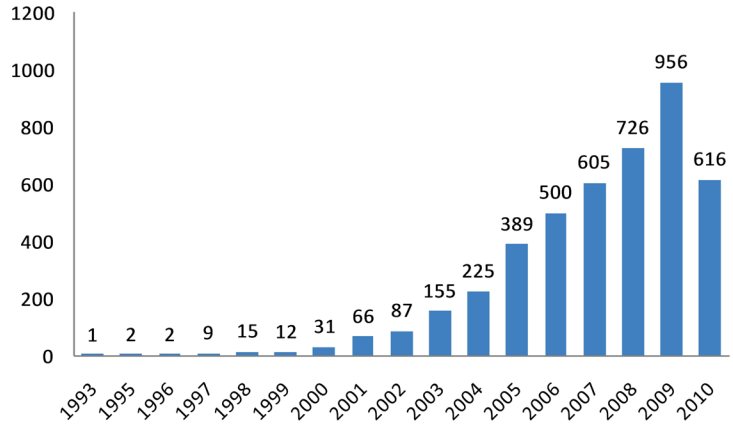

Fig. 16. Number of DSSC publications per year found under the search term "dye-sensitized solar cells" in SciFinder (June 19, 2010)

Side-chain porphyrin polymers

Tetraphenylporphyrins have been incorporated into conjugated polymer bulk heterojunction solar cells or in more elaborate supramolecular structures. An example is an organic solar cell device which organized fullerenes and porphyrins for efficient electron transfer through a polypeptide structure, resulting in a power conversion efficiency of 1.6% [96] (Fig. 15f). This configuration demonstrated a highly efficient IPCE = 56% using a composite cluster of free-base and zinc porphyrin structures.

DYE-SENSITIZED SOLAR CELLS

In 1991, O'Regan and Grätzel published a landmark paper on solar energy conversion using a device architecture now commonly referred to as a dye-sensitized solar cell (DSSC) or more simply the "Grätzel cell" [97]. The architecture is constructed using a conductive glass electrode, typically fluorine-doped tin oxide (FTO) covered with high surface area TiO_2 which is coated with a monolayer of light-harvesting dye molecules to make the photoanode. In order to complete the circuit, a counter electrode made of platinum-coated FTO is sandwiched on top of the photoanode. Finally, a thin layer of redox electrolyte (iodide/triiodide) is added to the inter-electrode space, making the final functional DSSC. The solar cell functions when a dye molecule is excited by light (a HOMO to LUMO transition), whereby the excited electron can be injected into the conduction band of TiO_2. The electron is then passed through the TiO_2 into the conductive glass substrate and into a circuit where the high-energy electron can be made to do useful work. Upon completion of useful work the low-energy electron passes through the counter electrode and is ferried back to the dye molecule via the redox electrolyte. Because the components of the cell are relatively inexpensive and the overall efficiency can be up to 11%, the DSSC has the potential to be a low-cost alternative to standard silicon photovoltaics. Since 1993, the number of publications on DSSCs has grown steadily reaching nearly 1,000 in 2009 (Fig. 16); the seminal paper published by O'Regan and Grätzel has been cited over 5,000 times (ISI Web of Knowledge, accessed 5/10/10).

The most common implementation of the DSSC uses ruthenium-based dyes. Unfortunately, ruthenium is not an earth-abundant element, and it is unlikely that the supply and/or cost of ruthenium will allow such DSSCs to be as widely adopted as needed for a true solar-based economy. In order to solve this problem extensive research has and is being done to replace the ruthenium sensitizer with a dye that can achieve the same or better efficiency while remaining inexpensive and easy to synthesize. Porphyrinoid molecules have received a great deal of attention in that regard because of their versatility, ease of construction, long-term stability, and relation to natural photosynthesis. The recent report of a porphyrin solar cell with 11% efficiency [98] has clearly shown that these compounds can match up with the best of sensitizers for DSSCs.

As early as 1993, natural porphyrins and chlorophylls were being studied in DSSCs [99, 100] and interest in these dyes has continued to grow. The five main tetrapyrrole structures that have been used in DSSCs are porphyrins, chlorins, bacteriochlorins, phthalocyanines, and corroles (Fig. 17). Porphyrinoid derivatives and their DSSC performances have been the subject of several reviews in the last few years covering most cyclic tetrapyrrole derivatives [101], porphyrins and phthalocyanines

Copyright © 2010 World Scientific Publishing Company

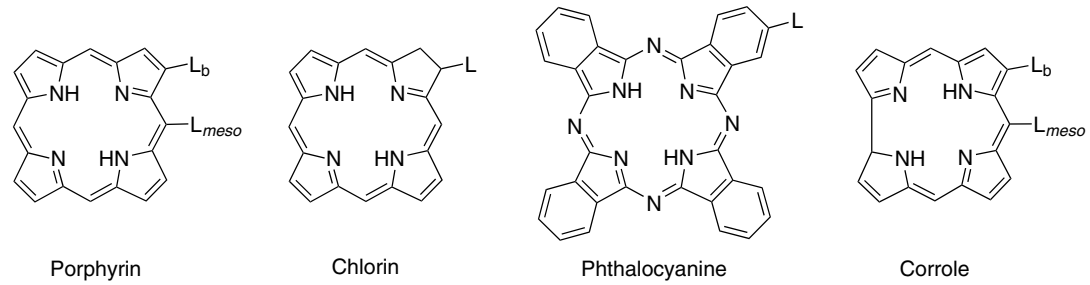

Fig. 17. General structures for the four main porphyrinoid light-harvesting dyes. A fifth dye type, the bacteriochlorin, is a chlorin in which two pyrrole rings opposite one another are reduced. L represents possible linker sites for attachment to the DSSC

[102, 103], and porphyrins by themselves [104]. Based on the structural diversity of porphyrinoid sensitizers a convenient way of organizing different dyes within a type is to distinguish between the placement and structure of binding groups used to adsorb the dye to the TiO_2 substrate. The different positions of some typical dye-linking groups within each type can be seen in Fig. 17, where L represents the linker. This approach will be used in this discussion to organize the different groups and is especially relevant for the porphyrin-based DSSCs, where the location and role of the linker group has been shown to be particularly important.

As can be seen from the complexity of DSSC construction there can be many ways to achieve optimization and improved efficiencies, including different selections and processing of the semiconductor, electrolyte, surface treatments, solvents, and miscellaneous additives. In each case much research has been done to manipulate each variable and in some cases an entire review paper could be written just on one aspect of cell construction. Our focus will be on the specific dyes – their structures and their performance in standard DSSCs (TiO_2 nanoparticles on FTO glass, platinum counter electrode, and iodide/triiodide electrolyte). Unless it appears unusual or relevant, little attention will be paid to differences in cell construction techniques and additives as these will vary greatly between research groups.

Porphyrins in DSSCs

The use of porphyrins in DSSCs was first demonstrated by Kay and Grätzel in 1993 [99, 100], and since that time the search for efficient porphyrin dyes for DSSCs have been a major focus of research. Since 2000, at least 378 publications have focused on the use of porphyrins in solar cells and the trend has been consistently growing (Fig. 18).

Based on the porphyrin structure there are two main points of attachment for TiO_2-linking groups, the *meso* and β positions (Fig. 17). Within the *meso*-position two main classes of linking moieties have been employed most often, the classic *meso*-substituted benzoic acid linking and the direct attachment of a *meso*-alkynylbenzoic acid moiety, a much newer focal point for porphyrin DSSC research. For DSSCs employing a β-position

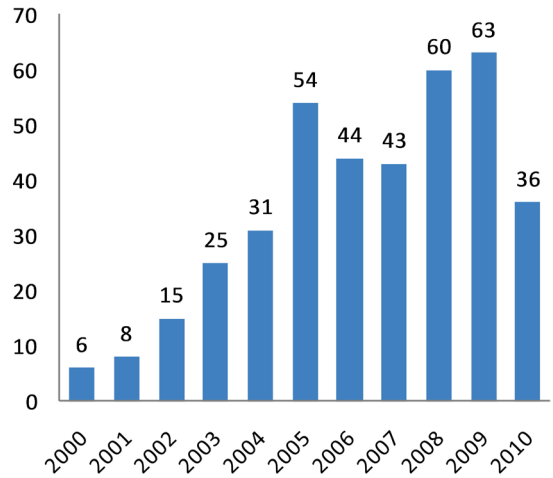

Fig. 18. Number of porphyrin solar cell publications per year found via the search term "porphyrin solar cells" in SciFinder (June 19, 2010); note that not all reports are necessarily of porphyrins in DSSCs

linking group only one clear distinction between dye attachment types can be made, the difference between conjugated and non-conjugated linkers. Conjugated linkers have received the most attention by far and as such the attention in this discussion will be focused on conjugated attachment methods. Since the majority of work on porphyrin DSSCs is focused on these three areas, they became natural delineators for the following compilation. Additional miscellaneous design strategies include other *meso*-based attachments, metal-ligand binding, porphyrin:C_{60} aggregates that bind to TiO_2, and design strategies that lead to solid-state DSSCs (DSSCs that lack the classic liquid electrolyte). Throughout, we use the same abbreviations for structures as appeared in the original literature to facilitate locating the compounds in the original literature.

Porphyrins anchored through meso-phenylcarboxy groups. DSSCs using porphyrins with *meso*-substituted benzoic acid linking groups are some of the earliest and still probably the most studied of the porphyrinoid-based sensitizers. A general structure for a *meso* tetrasubstituted porphyrin is given in Scheme 1. If R_1-R_4 are *para* benzoic acid moieties and M = 2H, we have 5,10,15,20-tetrakis(4-carboxyphenyl)porphyrin (TCPP), which has been studied as a model system in solar cells and as a

Copyright © 2010 World Scientific Publishing Company

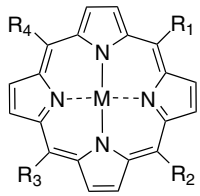

M = 2H or Zn

Scheme 1. General porphyrin structure

standard dye for over ten years [105–110]. Table 2 lists DSSC parameters for representative tetraphenylporphyrin sensitizers that use a *meso*-substituted benzoic acid moiety as binding group [105, 111–114]. As can be seen in Table 2, a number of different design aspects have been applied to *meso*-substituted porphyrin sensitizers.

Over the last decade, the efficiency values for *meso*-substituted benzoic acid-tethered porphyrins have not changed much. In 2000, free-base **TCPP** (Fig. 19) was reported at an efficiency of 3.5% under low light intensity [105]. That report also analyzed the adsorption properties of **TCPP** on TiO_2 using XPS and resonance Raman spectroscopy to elucidate the binding characteristics of **TCPP** and reported that low concentrations of dye in the adsorption solution (~0.1 mM) are important to avoid dye aggregation.

More recent work has studied mixed amino/carboxyphenylporphyrins, using the amino groups as possible nucleation points for polymerization of aniline to create solid-state solar cells [118]. Using 5-(4-aminophenyl)-10,15,20-tris(4-carboxyphenyl)porphyrin in a liquid electrolyte solar cell with a polyaniline counter electrode gave an overall efficiency of 1.1% [119]. The ability to create a variety of substituents on the porphyrin macrocycle has become very popular with the advent of simple synthetic methodology to *meso* tetrasubstituted porphyrins [120]. A useful purpose for lowered symmetry is to help electron injection by creating a strong dipole that facilitates electron transfer toward the LUMO of the macrocycle. A number of examples of asymmetric porphyrin-sensitized DSSCs are cited in Table 2.

In 2009, Imahori and co-workers studied a series of monocarboxyphenyl triaryl porphyrins in DSSCs [111]. The results of their work with zinc porphyrins can be seen in Table 2. In this group, the Zn porphyrin **2,4,6-Me** yielded the highest efficiency of 4.6% in a standard

Table 2. Substitution pattern and solar cell performances of *meso*-carboxyphenylporphyrin sensitizers in DSSCs

Attaching group (R_1)	R_2, R_3, R_4 groups	Lit. abbrev. [reference]	J_{sc}, mA/cm^2	V_{oc}, V	η, %
p-C_6H_4COOH M = 2H	*p*-C_6H_4COOH	**TCPP** [105]	0.170	0.46	3.5[a]
p-C_6H_4COOH M = Zn	*p*-C_6H_4COOH	***p*-ZnTCPP** [115]	0.390	0.44	1.1[b]
m-C_6H_4COOH M = Zn	*m*-C_6H_4COOH	***m*-ZnTCPP** [114][c]	3.33	0.51	0.69[b]
p-C_6H_4COOH M = 2H	C_6H_5	**uTPP** [113]	4.25[d]	0.62[d]	1.5
p-C_6H_4COOH M = 2H	*p*-$C_6H_4C_5H_{11}$	**uTPP-alkyl** [113]	7.75[d]	0.67[d]	3.2
p-C_6H_4COOH M = Zn	*p*-$C_6H_4CF_3$	**4-CF_3** [111]	6.6	0.67	3.0
p-C_6H_4COOH M = Zn	*p*-C_6H_4Me	**4-Me** [111]	8.3	0.68	3.8
p-C_6H_4COOH M = Zn	*p*-C_6H_4OMe	**4-OMe** [111]	8.3	0.66	3.5
p-C_6H_4COOH M = Zn	2,4,6-$Me_3C_6H_2$	**2,4,6-Me** [111]	9.4	0.76	4.6
p-C_6H_4COOH M = Zn	2,4,6-$Et_3C_6H_2$	**2,4,6-Et** [111]	8.6	0.69	3.7
p-$C_6H_4C_6H_4COOH$ M = Zn	2,4,6-$Me_3C_6H_2$	**BP** [111]	6.0	0.65	2.6

[a] Determined under low light intensity (1.4 mW/cm^2). [b] Calculated based on information given in the article. [c] Others have studied m-ZnTCPP [116, 117]. [d] Estimated from current-voltage curve.

Copyright © 2010 World Scientific Publishing Company

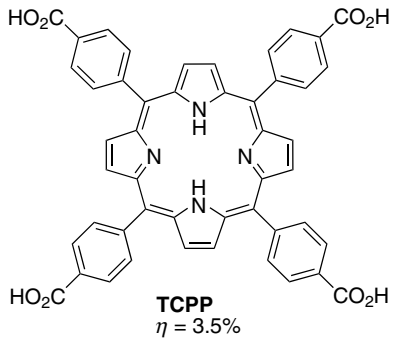

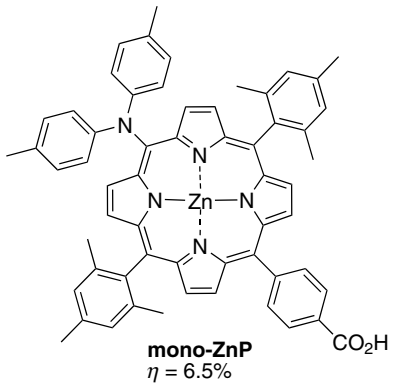

Fig. 19. Chemical structures of the most efficient free-base [105] and zinc-metallated [121] *meso*-substituted porphyrins having a benzoic acid linking group

DSSC. As a part of their study, Imahori *et al.* optimized the adsorption time and adsorption solvent for dye loading on TiO_2 films and determined that lower adsorption times and protic solvents (methanol) led to the best efficiencies. In more recent work, integration of a push-pull structure with a trans diphenylamino substituent gave a very high efficiency of 6.5% (Fig. 19, **mono-ZnP**) [121].

One issue with porphyrins as sensitizers in DSSCs is their limited absorptivity in the red and near infrared regions of the solar spectrum. With *meso*-tetraphenylporphyrins the phenyl moieties are typically considered perpendicular to the plane of the macrocycle and therefore are not in conjugation with the porphyrin π system. One design strategy for increasing the light absorption of porphyrin sensitizers is to lock the *meso*-phenyl ring into the plane of the macrocycle in order to improve the π-conjugation between the porphyrin and the phenyl rings. This strategy has the added benefit of increasing the molecular asymmetry of the molecule [122]. The combination of added π-conjugation and increased molecular asymmetry manifests itself as a red shift in the absorption spectrum of the molecule. Imahori and coworkers attempted this strategy with the dye **Fused-Zn-1** (Fig. 20). They found that the fused porphyrin absorption was red-shifted and broadened, and it was a more efficient sensitizer than the unfused analog (η = 4.1% versus 2.8%) under similar experimental conditions [122].

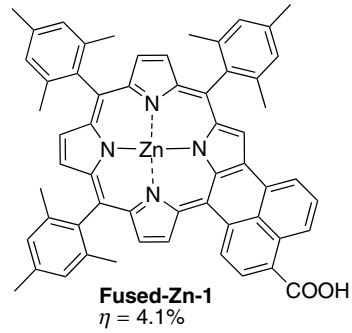

Fig. 20. A fused naphthalene porphyrin [122]

Although *meso*-carboxyphenyl tethered porphyrins have been studied a great deal in DSSCs, there remains a concern about the decoupling of the phenyl rings from the conjugated system of the macrocycle, which potentially limits the electronic communication between the excited dye and the linkage to the semiconductor. Recently, more attention has been paid to other structural designs such as porphyrins with *meso*-alkynylbenzoic acid or β-linked conjugated tethers; devices using these designs have reached remarkably high efficiencies.

Porphyrins anchored through meso-alkynylbenzoic acid groups. The use of *meso*-linked alkynylbenzoic acid tethers is a relatively new design strategy in porphyrin DSSC research. The first report of alkynylbenzoic acid-tethered porphyrins was by Stromberg *et al.* in 2007 [123] in which the reported photocurrent of the device was only 0.035 mA/cm^2. Since then two main groups (Dr. Joseph Hupp and Dr. Eric Diau) have studied this novel tether style and DSSC devices utilizing them. The use of the *meso*-alkynylbenzoic acid tether has led to an increase in solar cell efficiency for porphyrin DSSCs and even put forth a series of porphyrin dyes that outperformed the standard dye N719 under similar experimental conditions [124, 125].

It is worth noting that many DSSC studies not only report their laboratory-measured cell efficiencies (η), but also cite their measured efficiency of N719 dye as a relative standard of cell efficiency. Although N719 has been reported in cells operating at up to 11% efficiency [126], the variability of cell preparation in different labs often makes absolute efficiency comparisons difficult to compare (and very few labs can get N719 to operate at efficiencies that high). When absolute cell efficiencies are required, the National Renewable Energy Laboratory provides a certified measurement service [127].

In papers by Hupp and co-workers, dyes **1b** and **3** (Fig. 21) were reported to give efficiencies of 2.5 and 1.6% respectively in standard TiO_2 DSSCs [128, 129]. In the case of **1b**, a comparison with N719 was made and **1b** performed at ~71% the efficiency of N719. In the report on **1b**, ZnO was also tested as a semiconductor, and it was determined that the more acidic dyes that tend to slightly corrode the ZnO surface showed better electron injection dynamics. In the case of dye **3**, the use of

Copyright © 2010 World Scientific Publishing Company

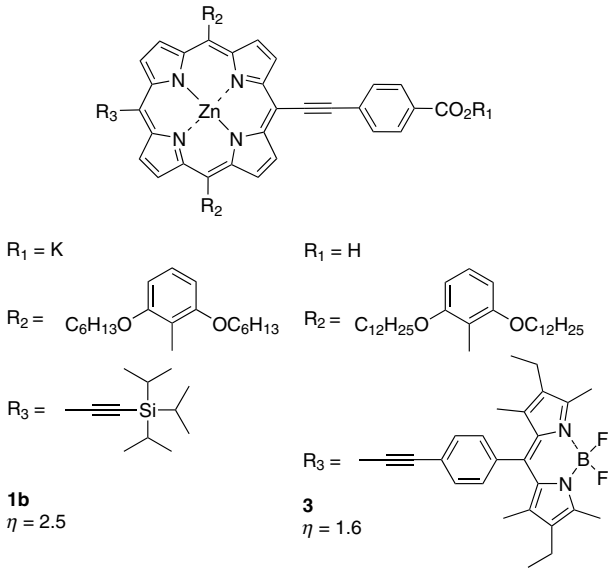

Fig. 21. Structures of two *meso*-alkynylbenzoic acid type porphyrin dyes and their efficiencies in DSSCs (**1b** [128], **3** [129])

a boron-dipyrromethene (bodipy) antenna chromophore resulted in an increase in device efficiency over a dye that did not contain the antenna complex.

A great deal of research into alkynylbenzoic acid tethers has been done by Diau and co-workers over the last several years. The structural design of this group of dyes takes the form of donor-porphyrin-π conjugated bridge-acceptor. A particularly successful donor group has been the diarylamino moiety. Several examples of this type of dye are given in Fig. 22, which depicts dye structures and efficiencies for the three highest-performing alkynylbenzoic acid dyes reported to date: dye **YD1** (6.4%), **YD2** (6.6%), and **YD12** (6.7%) [124, 125, 130]. Of high interest is the report that when N719 was compared to **YD1**, **YD2**, and **YD12** under similar experimental conditions, all three dyes outperformed N719 in cases where no scattering TiO_2 layer was used (N719 performed at 98%, 95% and 92% the efficiency of the porphyrin dyes, respectively). When a scattering layer was used, all cells improved in efficiency, but N719 then outperformed the porphyrin cells, with dyes **YD1**, **YD2**, and **YD12** giving 89%, 93% and 95% the efficiency of N719 [124, 125]. Most recently, **YD2** was tested in the Grätzel labs at EPFL and an optimized efficiency of 11% was obtained [98].

An example of a porphyrin dimer with a *meso*-alkynylbenzoic acid attaching group was reported by Diau and co-workers. The dye **YDD1** (Fig. 23) gave an efficiency of 5.2% in a standard DSSC [131].

In order to determine the effects of the bridging moiety length and the size of the intermediate acene, Diau and co-workers synthesized a series of dyes to probe each of these aspects of dye design [132–135]. A series of porphyrin dyes with differing numbers of ethynylphenyl groups (1–4) were produced and tested; the optimal

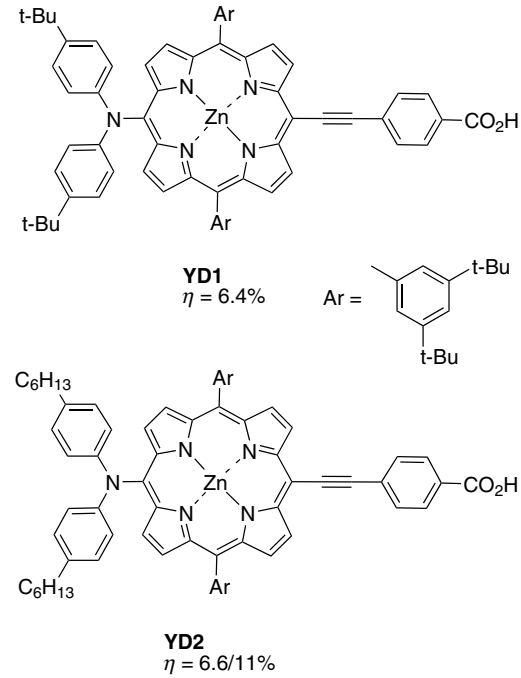

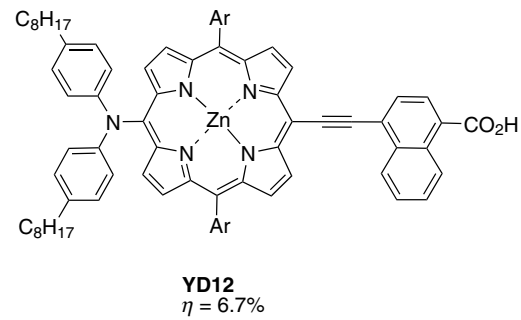

Fig. 22. Structures of three donor-bridge-acceptor porphyrin dyes and the effect of adding long alkyl chains to the donor moiety on DSSC efficiency (**YD1** [125], **YD2** [98, 125], and **YD12** [124])

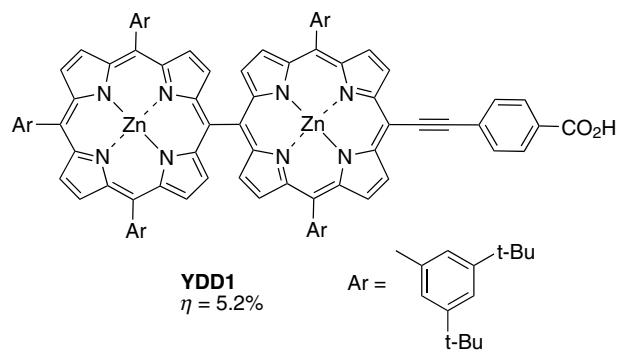

Fig. 23. A *meso*-linked porphyrin dimer with alkynylbenzoic acid linking group [131]

dye **PE1** (with n = 1) is shown in Fig. 24a and gave an efficiency of 2.7% [133]. To probe how the number of aromatic rings in the bridging group affects solar cell performance, a series of porphyrin dyes with benzene

Copyright © 2010 World Scientific Publishing Company

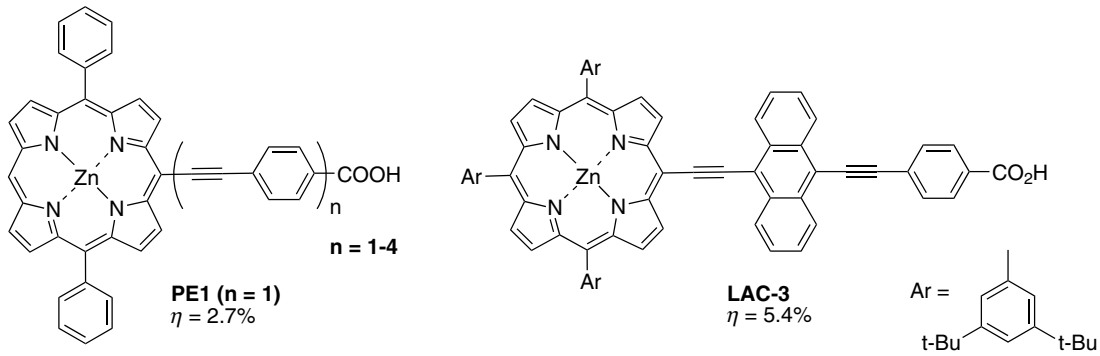

Fig. 24. Optimization of (a) alkynylbenzoic acid tether length [133] and (b) acene modification of tether groups [134] and the DSSC efficiency of the optimum structures

through pentacene moieties were synthesized and tested as DSSCs. The optimal dye (**LAC-3**) is shown in Fig. 24b and gave an efficiency of 5.4%; under similar conditions, N719 gave an efficiency of 6.7% [134].

Other meso-linked porphyrin dyes. Porphyrin dyes with other *meso* attachment methods take several novel forms. One example is the use of directly *meso*-linked thiophenyl and furanyl-carboxy binding moieties as was demonstrated by Eu *et al.* [136]. The dyes **Zn5S**, **Zn4S**, and **Zn5O** (Fig. 25) gave efficiencies of 3.1, 1.8 and 2.3%, respectively. The difference between **Zn5S** and **Zn5O** is attributed to the possibility of a secondary electron transfer pathway between the sulfur atom on the binding moiety and the TiO_2 surface. The low η of **Zn4S** may have been due to its much lower adsorption rate onto the semiconductor surface.

Research by Liu and co-workers has focused on adding thiophenyl groups to the *para*-position of *meso*-phenyl groups with and without a specific binding functionality (*i.e.* –COOH). Dye $\mathbf{P_{Zn}}$**-hT** (Fig. 25) gave an efficiency of 5.1% when DMF was used as the adsorption solvent [137], which was 64% of the performance of N719 under comparable conditions. Liu *et al.* also produced a porphyrin dye with polythiophene moieties (seven repeat units) attached to each *meso*-phenyl group *para*-position (**P-bs2**, Fig. 25), which they called porphyrin-polythiophene stars [95], **P-bs2** gave an efficiency of 3.9% when chenodeoxycholic acid was used as a co-adsorbent in a DSSC. The lack of a typical binding moiety in the **P-bs2** dye leaves open the question of how the dye is adsorbing to the TiO_2 surface. One possible answer is that the sulfur atoms of the thiophene groups may be interacting with the TiO_2 surface and that electron injection may follow the same secondary path mentioned earlier by Eu *et al.* [136].

A porphyrin dimer by Officer and co-workers, **P10**, gave an efficiency of 3.8% when used in a DSSC (Fig. 25) [138]. The dimer consists of two zinc porphyrins connected through a conjugated β to *meso*-linkage and a binding moiety that combines a *meso*-phenyl group with a cyanoacrylic acid via attachment to the phenyl *para*-position. As can be seen from Fig. 25, the connection between the two porphyrins in the dimer was *trans* to the binding group. A related dye reported by the same group with *cis* geometry between the second porphyrin and the binding group gave a lower efficiency of 3.1% [138].

Other notable *meso*-tethered porphyrin dyes include a direct *meso*-linked cyanoacrylic acid group and the use of N-acetic acid Rhodamine binding moieties attached to the *para*-position of *meso*-phenyl groups (two binding groups attached in *trans* geometry). In the former, a respectable J_{sc} of 7.6 mA/cm^2 was reported, but few details of other solar cell performance parameters were given [123]. The latter gave a DSSC efficiency of 0.76% [139, 140].

Beta-linked anchoring groups. The use of conjugated β-substituted anchoring groups was first demonstrated in 2004 by Nazeeruddin *et al.* when they introduced a dye with an energy conversion efficiency of 4.1% [141]. Since then β-substituted porphyrins have achieved efficiencies greater than 7% and have been synthesized to study substituent effects [142, 143], to probe different aspects of cell design [144, 145], and to elucidate the origin of specific limitations to photovoltaic properties (*e.g.* open circuit voltage and injection dynamics) [146, 147]. Scheme 2 shows a generic porphyrin structure with the variable substitution positions R and R_1, where R is the site of the β-linkage. Table 3 displays some of the β-substituted porphyrins that have been tested in DSSCs, their photovoltaic performances, the original reference, and the abbreviation for the compound as it appears in the original publication (however, see note at the bottom of Table 3).

In 2007, Officer and co-workers reported a 7.1% efficient porphyrin, the dye cited as **2** in Table 3, which consisted of a tetratolylporphyrin with a conjugated bridge to a dicarboxylic acid acceptor moiety (Fig. 26) [142]. This work included a series of porphyrin dyes; the top three performing dyes are shown in Fig. 26, all of which are over 6% efficient. Grätzel and co-workers also used dye **2** in a solid-state device that will be discussed later.

Since the 2007 report on β-linked porphyrins, Officer and co-workers have used β-linked derivatives to study several aspects of solar cell design and performance. The aspects of design under study included the use of a post-adsorbed phosphinic acid blocking moiety to improve

Copyright © 2010 World Scientific Publishing Company

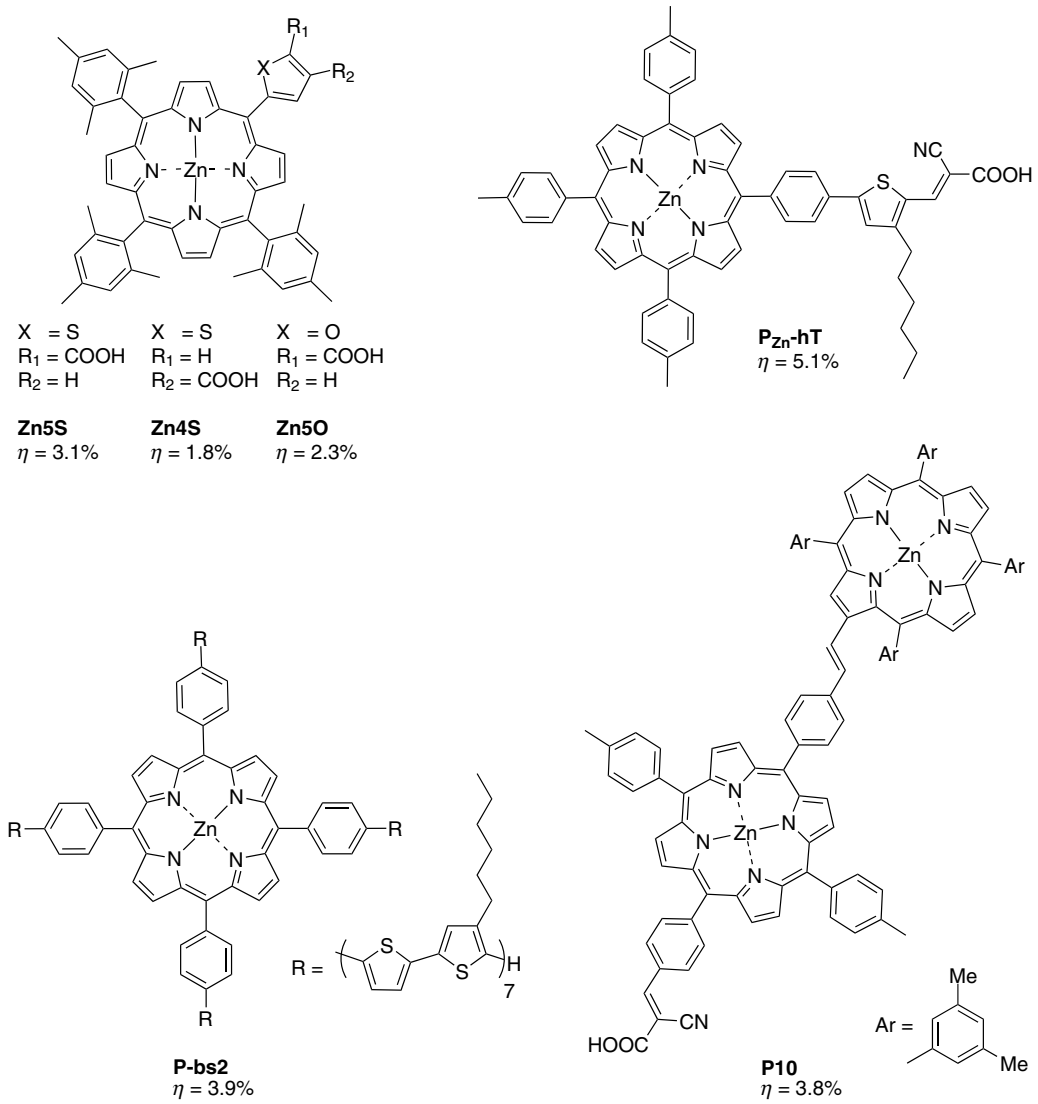

Fig. 25. Porphyrin structures with other *meso*-linkages and their efficiencies in DSSCs (**Zn5S, Zn4S, and Zn5O**) [136], **P_{Zn}-hT** [137], **P-bs2** [95], and **P10** [138])

efficiencies by minimizing recombination events at the electrode surface [144]. They also studied the use of ionic liquid electrolytes as a replacement for volatile organic solvents in typical liquid electrolytes [145]. The Officer group has also studied the open-circuit voltage and electron injection dynamics using β-substituted porphyrins and have suggested that the reason for limitations to the V_{oc} and J_{sc} are related to reduced electron lifetime and less favorable electron injection dynamics [146, 147].

Imahori and co-workers reported novel β-linked porphyrins with carboxyquinoxalino or dicarboxyquinoxalino moieties. The carboxyquinoxalino dye (**ZnQMA**) is shown in Fig. 27 [148]. **ZnQMA** gave a solar energy conversion efficiency of 5.2% in a standard DSSC, while the dicarboxy derivative (**ZnQDA**) gave 4% efficiency. The better efficiency of **ZnQMA** was attributed to better electron injection and charge collection efficiency [148].

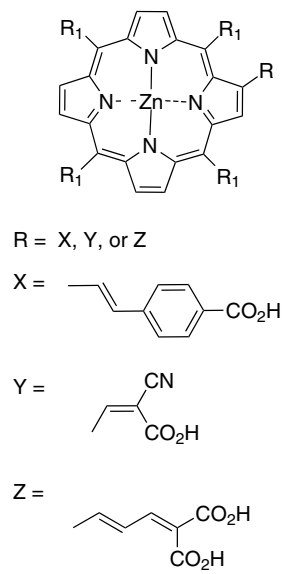

Scheme 2. General *beta*-linked porphyrin structure

Copyright © 2010 World Scientific Publishing Company

Table 3. Substitution pattern and performances of β-linked porphyrin sensitizers in DSSCs (see Scheme 2 for the position of groups R and R_1 on the porphyrin macrocycle)

Attaching group (R)	R_1	Lit. abbr. [reference]	J_{sc}, mA/cm^2	V_{oc}, V	η, %
X	C_6H_5	**Dye-1** [141][a]	8.86	0.65	4.1
X	*p*-MeC_6H_4	**Dye-2** [141][a]	9.70	0.66	4.8
Y	C_6H_5	**Zn-3** [143]	13.5	0.57	5.6
Z	*p*-MeC_6H_4	**2** [142]	14	0.68	7.1
Z	*p*-BuC_6H_4	**4** [142]	13.4	0.70	6.4
Z	3,5-$Me_2C_6H_3$	**6** [142]	13.3	0.69	6.1

[a] Called **1** and **2** in the original reference.

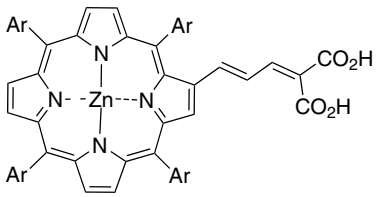

2 (Ar = p-MeC$_6$H$_4$)
η = 7.1%

4 (Ar = p-BuC$_6$H$_4$)
η = 6.4%

6 (Ar = 3,5-Me$_2$C$_6$H$_3$)
η = 6.1%

Fig. 26. Porphyrin structures for the most efficient group of β-linked porphyrins and their performances in DSSCs [142]

A novel *meso-meso* dimer with two *cis* conjugated β anchors was reported by Park *et al.* The dye **PEG-2b-bd-Zn2** gave an efficiency of 4.2% in a standard DSSC (Fig. 27) [149]. The report included several other interesting *meso-meso*-linked porphyrins that gave efficiencies between 3 and 4%.

Other novel dye attachment methods. Porphyrins have been incorporated into DSSCs using a variety of creative and interesting attachment methods; a brief representative sampling is given here. A metalloporphyrin was fitted with an axial ligand that included an anchoring moiety to bind to TiO_2 (see Fig. 32 for an analogous situation using a phthalocyanine dye) [150]. Other metal-ligand combinations have been used to form networks of dyes for DSSCs [151]. Donor-acceptor clusters, such as fullerene-porphyrin clusters, have been aggregated onto gold nanoparticles via thiol groups and used as dyes for DSSCs (see Fig. 10 for a representative example) [54, 66, 152, 153].

Solid-state DSSCs. The use of liquid electrolytes in DSSCs is considered one of the main limitations of these devices, primarily due to issues with containment [142]. Work to replace the liquid electrolyte with a solid hole-transport medium has been undertaken by several research groups. One of the first porphyrin-based solid-state DSSCs was reported by Zhang and Xiao in 2000 [154]. The device was made up in the following order: SnO_2/TiO_2/TCPP/CuI/Al with CuI acting as the solid hole transporter. The J_{sc} and V_{oc} of the device were 46 μA/cm^2 and 0.051 V, respectively. More recent work by Kang *et al.* and Giribabu *et al.* has focused on the use of quasi solid-state polymer gel electrolytes in porphyrin DSSCs with cell efficiencies of 2.8% and 0.38% when polyethylene glycol and polyacrylonitrile were used as the polymer base of the gel respectively [140, 155]. Officer and co-workers used a β-linked porphyrin (dye **2**, Fig. 26) in a solid-state device with *spiro*-MeOTAD as the hole-transport medium; the device gave an overall efficiency of 3.6%.

In research done by Wamser and co-workers, the device displayed in Fig. 28 was constructed in which polyaniline was generated *in situ* via photoelectrochemical polymerization of aniline. The device gave an efficiency of 0.8%

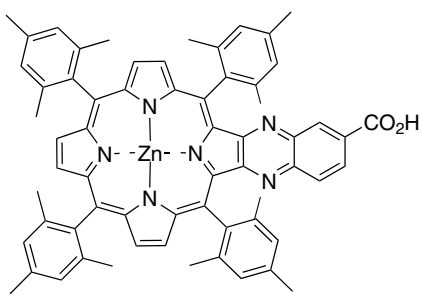

ZnQMA
η = 5.2%

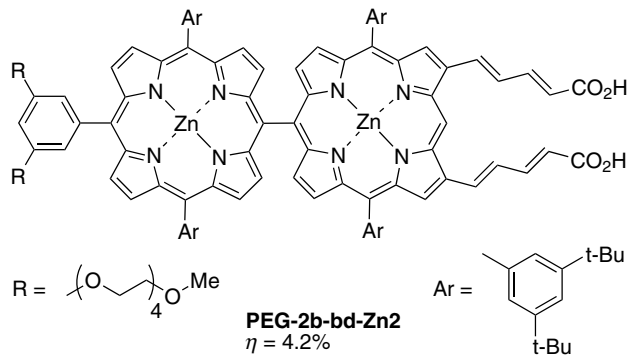

PEG-2b-bd-Zn2
η = 4.2%

Fig. 27. Structures for two other novel β-linked porphyrins (**ZnQMA** [148] and **PEG-2b-bd-Zn2** [149])

Copyright © 2010 World Scientific Publishing Company

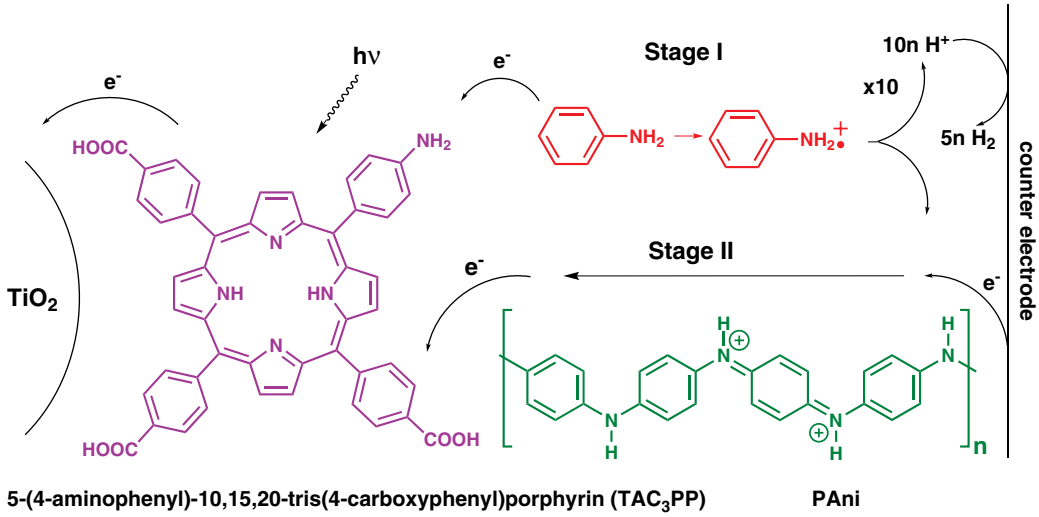

Fig. 28. Solid-state DSSC using an amino/carboxyphenylporphyrin and employing polyaniline as a novel hole-transport medium, with the proposed mechanism of polyaniline synthesis (Stage I) and electron transport (Stage II) [119]

under low light intensity. The proposed mechanism is outlined [119].

Chlorins and bacteriochlorins in DSSCs

The use of chlorins in a DSSC was first reported in 1993 by Kay and Grätzel [99, 100]. In that report a variety of metallo and free-base carboxychlorins were produced from natural chlorophylls via metallation and/or saponification. The best DSSC reported was a copper chlorophyll derivative, Cu-chlorin e_6 (see Fig. 29), which gave an overall energy conversion efficiency of 2.6%. Since this first report, **chlorin-e$_6$** has been studied in DSSCs using both its free-base [156] and zinc-metallated [157] forms as well as being used as a model system for studies comparing the effectiveness of different types of co-adsorbents [158, 159]. The best performance of a DSSC using **chlorin-e$_6$**, η = 4.3%, was reported in 2007 by Ikegami and co-workers [160] (Fig. 29) and came about after optimizing the co-adsorbent to avoid molecular aggregate formation between dye molecules.

Further advances in the use of chlorins and bacteriochlorins have necessitated the development of synthetic methodologies to build stable macrocycles and modify existing structures with linking groups that will bind TiO_2 [123]. The Lindsey group has advanced such a methodology and has used it to synthesize novel chlorin and bacteriochlorin derivatives substituted at the *meso*-position with ethynylisophthalic acid linking groups. Although overall power conversion efficiencies were not reported, J_{sc} values for the chlorin and bacteriochlorin were relatively low (0.99 and 1.6 mA/cm^2, respectively), indicating that further structural optimization is necessary for these derivatives to be competitive [123].

The research by Wang and co-workers over the last several years has had a profound impact on advances in chlorin and bacteriochlorin DSSCs, starting in 2006 with work on chlorin **PPB *a*** in which an efficiency of 4.2% was achieved using β-carotene as a co-adsorbent (Fig. 29) [161]. Later **PPB *a*** was tested without the presence of the co-adsorbent and compared to other chlorins, bacteriochlorins, and porphyrins; in these tests, an efficiency of 3.8% was achieved and the **PPB *a*** was the best

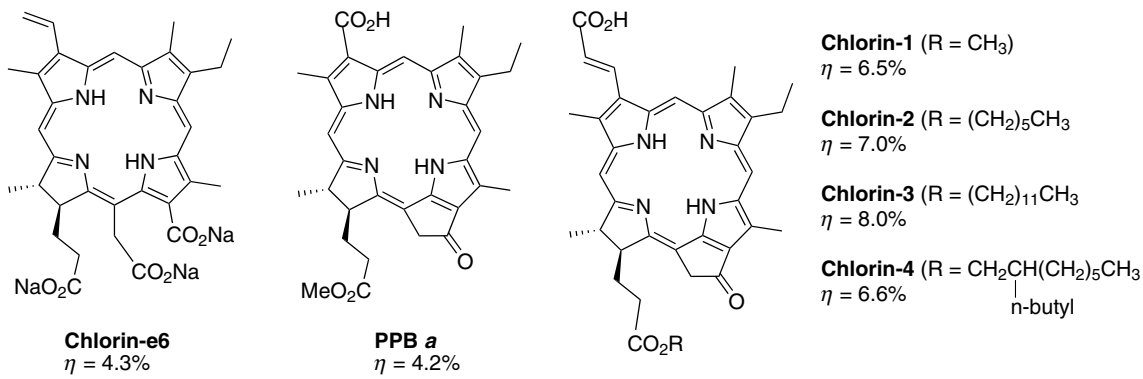

Fig. 29. Representative structures of chlorin derivatives and their efficiencies in DSSCs (**Chlorin-e$_6$** [160], **PPB a** [161], and **Chlorin-1-4** series [163])

Copyright © 2010 World Scientific Publishing Company

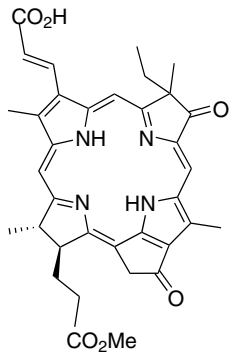

BChlorin-1
η = 6.2%

Fig. 30. Structure of a bacteriochlorin dye and its efficiency in a DSSC [165]

sensitizer tested [162]. More recent research has focused on chlorin and bacteriochlorin sensitizers that contain a conjugated linker. The **Chlorin-1-4** series (Fig. 29) have carboxylic acid groups linked to the chlorin macrocycle via an ethylene moiety and gave efficiencies in the range of 6.5% to 8% in DSSC tests, comparable to N719 which gave η = 9.3% under the same experimental conditions [163]. An improved efficiency of 7% has been reported for **Chlorin-2** [164]. **Chlorin-3** gave an overall efficiency of 8%, the best energy conversion efficiency to date for a chlorin sensitizer [163].

Recent work on bacteriochlorin sensitizers by Wang and co-workers has yielded the most efficient bacteriochlorin DSSC to date. The dye **BChlorin-1** (Fig. 30) uses dialkyl substitution at its second reduced pyrrole ring to increase the stability of the bacteriochlorin skeleton and avoid oxidation to the corresponding chlorin (a general problem with bacteriochlorins). The efficiency of **BChlorin-1** sensitized DSSC was found to be 6.2% and was improved to 6.6% when chenodeoxycholic acid was used as a co-adsorbent [165].

Phthalocyanines in DSSCs

Phthalocyanines (Pcs) are interesting candidates for sensitizers in DSSCs because of their strong red and near-IR absorbance, high extinction coefficients, good thermal, chemical, and photolytic stability, and easy tunability through rational design of the macrocycle structure [166–168]. Phthalocyanines have been used in solar cells with predominantly three different attachment methods: adsorption without any specific anchoring groups, anchoring using carboxy or sulfoxy substituents, and metal-ligand interactions in which the ligand bears the attaching group.

Phthalocyanine dyes without anchoring groups. Phthalocyanines in DSSCs in which no anchoring groups are involved take two forms. In the standard approach, physical adsorption occurs directly from solution onto previously sintered TiO_2 nanoparticles [169–171]. In the second method, the dye is physically adsorbed onto TiO_2 nanoparticles using powder-coating methodology and the resulting nanoparticles are made into a paste and applied to a layer of sintered TiO_2 using the doctor blade method to form TiO_2/dye composite particles [172, 173]. In both cases cell performance was very low (<1% efficiency), most likely due to the limited amount of phthalocyanine that can be physically adsorbed and the lack of good electronic connectivity with the semiconductor surface.

Phthalocyanine dyes with anchoring groups. Using Pcs with specific anchoring groups is the most common form of dye sensitization in phthalocyanine DSSCs [166–168, 174–179]. The most typical anchoring moiety is the carboxy group, which can be directly on the macrocycle or tethered to the macrocycle with a conjugated or non-conjugated linker. For example, the amino acid tyrosine was linked to the Pc macrocycle, exposing the carboxy end of the tyrosine as the anchoring group [179]. The tyrosine-linked Pc gave a low efficiency (0.54%), which may have been caused by dye aggregation and electron recombination with oxidized dye molecules. Sulfoxy linking groups have been reported before as well. In a novel solar cell by Balraju *et al.*, the dye **FeTsPc** was reported to give 3.1% efficiency with a PEDOT:PSS-coated FTO counter electrode (Fig. 31). Further improvement of the **FeTsPc** system was achieved when the TiO_2 surface was pretreated by dipping in dilute HNO_3 and water rinsing; the acid-modified cell gave an overall efficiency of 4.1% [176].

A great deal of work on Pc DSSCs has been done by Torres and co-workers, such as dye **2** (Fig. 31) with a conjugated naphthylcarboxylic acid linker that gave an efficiency of 2.2% [167]. Dye **TT1** gave an energy conversion efficiency of 3.6% when used with chenodeoxycholic acid as co-adsorbent (Fig. 31) [175] and 7.7% when used in a molecular cocktail DSSC with a triarylamine-dithiophene-acrylate donor/bridge/acceptor system as a co-sensitizer. The use of phthalocyanines with co-sensitizers is a novel way to engineer DSSCs that cover a wider range of the solar spectrum than can be accomplished with a single dye in a DSSC.

Imahori and co-workers reported a novel Pc sensitizer, **ZnPc**, which has two symmetric carboxy binding groups on one side of the molecule and the other free positions around the macrocycle substituted with bulky 4-*tert*-butylphenyl moieties to avoid aggregation (Fig. 31) [168]. The efficiency of **ZnPc** was shown to be 0.57% with and without the addition of a co-adsorbent, which implies that the substitution with bulky groups helped avoid aggregate formation and made a co-adsorbent unnecessary. The synthetic design was notable in that only one regioisomer was present in the final dye, a factor often hard to control in Pc synthesis.

The use of Pc dyes with two carboxy ligands that are not conjugated with the macrocycle core was demonstrated by Reddy *et al.* [177] The dye **PCH001** (Fig. 31) gave a maximum efficiency of 3.1% in the presence of chenodeoxycholic acid. The improved efficiency over a

Copyright © 2010 World Scientific Publishing Company

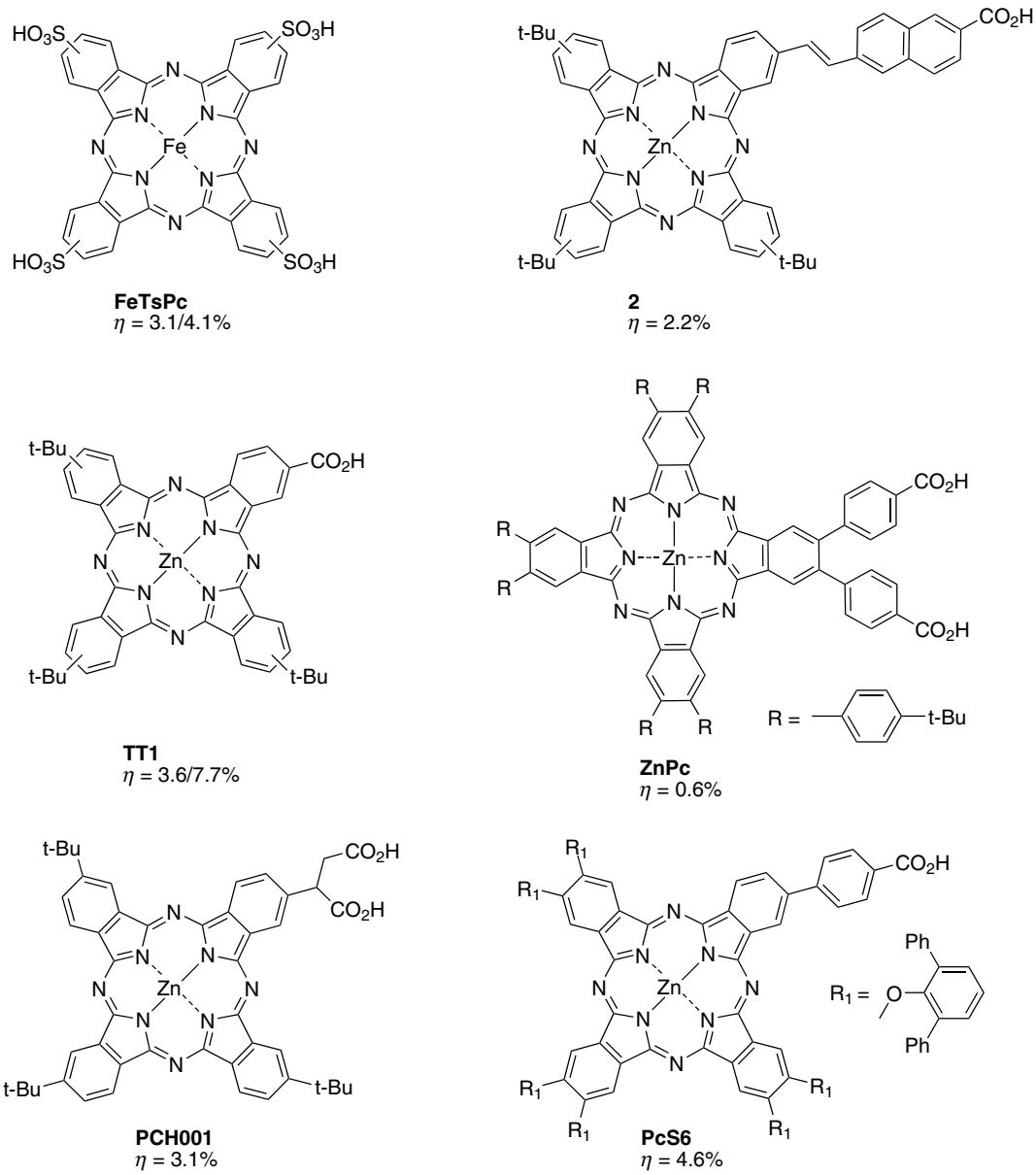

Fig. 31. Representative sample of phthalocyanine dyes and their efficiencies in DSSCs (**FeTsPc** [176], **2** [167], **TT1** [175], **ZnPc** [168], **PCH001** [177], and **PcS6** [178])

related tetracarboxy Pc was attributed to a lack of aggregation between neighboring Pc molecules and tight TiO_2 binding by the two carboxylic acid groups. A solid-state DSSC using **PCH001** and spiro-MeOTAD as the hole-transport medium gave an efficiency of 0.87% with a high V_{oc} of 0.72 V.

The highest efficiency DSSC using solely a phthalocyanine was reported by Mori *et al.* [178] **PcS6** (Fig. 31) gave a conversion efficiency of 4.6% which was two-thirds as efficient as an N719 cell tested under similar conditions. **PcS6** is a dye with a benzoic acid linking group on one side of the molecule, with all other positions substituted with a 2,6-diphenylphenoxy substituents (except the position vicinal to the attaching group). The steric bulk of the large diphenylphenoxy moieties apparently results in very little dye aggregation. Because the dye molecules are so large, some current may have been lost to recombination events between I_3^- at the TiO_2 surface, and future design strategies suggested by the authors may entail addition of blocking functionality [178].

Phthalocyanine attachment through axial metal-ligand interactions. The use of axial carboxylated ligands as binding moieties for phthalocyanines in DSSCs has been demonstrated several times over the last few years by Durrant and co-workers [180–182]. A typical dye-ligand system is shown in Fig. 32. The dye **RuPc3** gave J_{sc} of 3 mA/cm^2 and V_{oc} of 0.38 V. Note that the triarylamine ligand is positioned to serve as an electron donor. The only reported efficiency from one of these devices was 0.2% efficiency reported in 2004 [182]. One interesting result of this type of dye attachment method is the reduction of dye aggregation which is a common problem in

Copyright © 2010 World Scientific Publishing Company

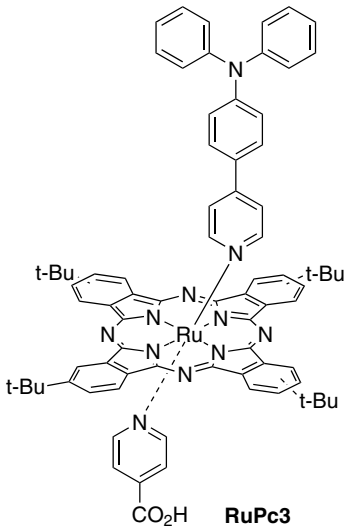

Fig. 32. Novel TiO_2 attachment method for a phthalocyanine dye [181]

phthalocyanine solar cells; more recent work suggests that there may be issues with recombination losses [181].

Another interesting axial ligand type Pc solar cell is one in which a Pc is attached through an axial ligand to a bis(bipyridyl)ruthenium (II) complex [183]. A low dye loading is cited to explain the relatively low overall efficiency of 0.34% as compared to N719 which gave an efficiency of 1.0% under similar conditions.

Corroles in DSSCs

Corroles are contracted porphyrinoid derivatives, having one less *meso*-position on the aromatic macrocycle. They are also a relatively new class of dyes to be used in DSSCs. There are only two literature references dealing with their performance in a DSSC, both referring to the work done in collaboration between Dr. Harry Gray and Dr. Zeev Gross [184, 185] in which a series of *beta*-disulfonated corroles with *meso*-pentafluorophenyl groups were tested in DSSCs. The best of the group, a gallium derivative, **GaC** (Fig. 33), gave an overall efficiency of 1.6%, roughly half the efficiency of N3 dye (a close relative of N719 dye) tested under similar conditions [184]. The major reason for the difference was a J_{sc} value that was half as large as the value cited for N3, with the V_{oc} and fill factors of the devices being comparable. The big difference in J_{sc} may be due to poor electron injection dynamics between the corrole LUMO and the conduction band of the TiO_2, possibly brought on by the use of sulfonyl binding groups rather than the more usual carboxyl groups.

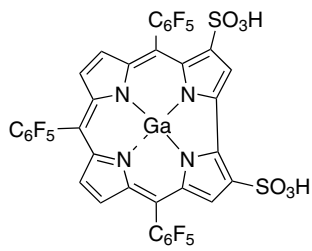

GaC
η = 1.6%

Fig. 33. Gallium corrole dye and its efficiency in a DSSC [184]

FUTURE PROSPECTS

New synthetic methodologies

In almost any area of chemistry, it is easy to predict that new synthetic capabilities will open up new possibilities. Synthesis of new porphyrins, phthalocyanines, corroles, chlorins, and more exotic macrocycles are regularly celebrated in this journal, but relatively few are explicitly tested in solar cells. Testing new compounds in solar cells is relatively routine, and collaborations between synthetic chemists and solar photochemists should be similarly routine. For example, recent methodology to carboxylate the *beta*-position of the corrole macrocycle [186] should open up the relatively quiet area of corrole DSSCs. Based on studies with porphyrins and other dyes, carboxy linkages should lead to stronger TiO_2 binding and better electron injection [185]. Many of the successful linking moieties that have been used with porphyrins then can be mirrored with corroles.

Improving light harvesting

Important synthetic targets should include porphyrins and related structures with a better match to the solar spectrum, especially stronger absorption into the red and near-infrared region. Dyes that may have been prepared for other purposes, yet show desirable solar spectral properties, should be modified to make them suitable as dyes for solar cells. For example, the phenomenally long-wavelength absorption of an azulene-fused porphyrin derivative (with absorption out to 1100 nm) [151] could be modified to incorporate carboxy groups and would serve as a very interesting DSSC dye.

Porphyrins and phthalocyanines absorb strongly in different parts of the visible region (Fig. 1), and co-sensitization strategies may be able to take advantage of each of them independently. Although co-sensitization has been shown to be effective in some cases, as with phthalocyanine TT1 (Fig. 31) [175], quenching of excited states without effective charge separation is a legitimate concern.

Optimizing HOMO/LUMO energies and electron distributions

In general, successful dyes employ a push-pull nature in the transition from ground state to excited state. In the ruthenium dyes, this is a charge-transfer excited state, in which an electron is excited from a Ru d orbital into a

Copyright © 2010 World Scientific Publishing Company

bipyridyl ligand π* orbital. Effectively, the electron is moved onto the ligand that is attached to the ultimate electron acceptor, and charge separation is facilitated. The analog of this process in a porphyrin or related organic dye is represented by the donor-bridge-acceptor structure of the most successful dyes. Essentially the HOMO should reside on the donor portion while the LUMO resides on the acceptor portion. Push-pull excitation creates an electron-hole pair at opposite sides of the molecule. As long as the directionality is right – the electron is moved towards the interface connected to the photoanode and the hole towards the interface connected to the photocathode – then the overall efficiency of charge separation can be enhanced. A number of computational studies have examined various porphyrin derivatives with this end in mind. Although most studies examine substituent effects on energy levels and HOMO/LUMO electron distributions in the porphyrin rings [187–189], some explicitly address the relative success of *beta*-linkages in redistributing electron density in the LUMO [190, 191].

Engineering interfacial nanostructures

Effective charge separation and charge collection require an interfacial structure with high surface area (to optimize excitons collecting efficiently at the interfaces, where charge separation takes place) as well as good continuity and conductivity in each of the phases (where charges are created and sent to the collecting electrodes). The material manipulation techniques of nanoscience have greatly improved the ability to design optimal structures that satisfy these often conflicting requirements. Highly ordered materials such as liquid crystals generally assist both exciton mobilities as well as charge mobilities, but generating a second continuous phase to interpenetrate the liquid crystal phase is still a challenge. Ordered nanostructures of TiO_2, to replace the nanoparticles typically used in DSSCs, has become a major area of research interest [116, 192, 193].

CONCLUSION

Porphyrins and their relatives have always presented an attractive array of optical and chemical properties. Applications in solar cells are a natural function for these compounds, and they have been extensively investigated in a variety of formats. Recent studies show that porphyrins can match the success of the best of dyes.

Acknowledgements

Financial support to CCW from the National Science Foundation (Grant CHE-0911186) and the Oregon Nanoscience and Microtechnologies Institute (ONAMI) is gratefully acknowledged. MGW was supported in part by an NSF American Competitiveness in Chemistry Postdoctoral Fellowship (Grant CHE-0937048). ABR was supported in part by an award from the Department of Energy (DOE) Office of Science Graduate Fellowship Program (DOE SCGF). The DOE SCGF Program was made possible in part by the American Recovery and Reinvestment Act of 2009. The DOE SCGF program is administered by the Oak Ridge Institute for Science and Education for the DOE. ORISE is managed by Oak Ridge Associated Universities (ORAU) under DOE contract number DE-AC05-06OR23100. All opinions expressed in this paper are the authors' and do not necessarily reflect the policies and views of DOE, ORAU, or ORISE.

REFERENCES

1. Milgrom LR. In *The Colours of Life: An Introduction to the Chemistry of Porphyrins and Related Compounds,* Oxford University Press: New York, 1997.
2. *Photosynthesis in Relation to Model Systems*, Vol. 3, Barber J. (Ed.) Elsevier Scientific Publishing Company: Amsterdam, 1979.
3. *Basic Research Needs for Solar Energy Utilization*, Lewis NS and Crabtree G. (Eds.) Office of Science: U.S. Department of Energy, 2005.
4. Bard AJ and Fox MA. *Acc. Chem. Res.* 1995; **28**: 141–145.
5. Hambourger M, Moore GF, Kramer DM, Gust D, Moore AL and Moore TA. *Chem. Soc. Rev.* 2009; **38**: 25–35.
6. Nelson J. In *The Physics of Solar Cells*, Imperial College Press: 2002; pp 17–39.
7. Imahori H. *J. Phys. Chem. B* 2004; **108**: 6130–6143.
8. Kodis G, Terazono Y, Liddell PA, Andreasson J, Garg V, Hambourger M, Moore TA, Moore AL and Gust D. *J. Am. Chem. Soc.* 2006; **128**: 1818–1827.
9. *Organic Photovoltaics: Mechanisms, Materials, and Devices*, Sun S-S and Sariciftci NS. (Eds.) Taylor & Francis: Boca Raton, FL, 2005.
10. Grätzel M. *Inorg. Chem.* 2005; **44**: 6841–6851.
11. Sun Q, Dai L, Zhou X, Li L and Li Q. *Appl. Phys. Lett.* 2007; **91**: 253505.
12. Walter MG and Wamser CC. *J. Phys. Chem. C* 2010; **114**: 7563–7574.
13. *The Porphyrin Handbook*, Kadish KM, Smith KM and Guilard R. (Eds.) Academic Press: San Diego, 2000.
14. Hoth CN, Schilinsky P, Choulis SA and Brabec CJ. *Nano Lett.* 2008; **8**: 2806–2813.
15. Tang CW. *Appl. Phys. Lett.* 1986; **48**: 183.
16. Kippelen B and Bredas J-L. *Energy Environ. Sci.* 2009; **2**: 251–261.
17. Gledhill SE, Scott B and Gregg BA. *J. Mater. Res.* 2005; **20**: 3167–3179.
18. Kietzke T. *Adv. Opto. Elect.* 2007; **40285**: 1–15.
19. Hains AW, Liang Z, Woodhouse MA and Gregg BA. *Chem. Rev.* 2010: DOI:10.1021/cr9002984.

Copyright © 2010 World Scientific Publishing Company

20. Scharber MC, Muehlbacher D, Koppe M, Denk P, Waldauf C, Heeger AJ and Brabec CJ. *Adv. Mater* 2006; **18**: 789–794.
21. Winder C, Matt G, Hummelen JC, Janssen RAJ, Sariciftci NS and Brabec CJ. *Thin Solid Films* 2002; **403–404**: 373–379.
22. Werner JH, Kolodinski S and Queisser HJ. *Phys. Rev. Lett.* 1994; **72**: 3851–3854.
23. Huijser A, Suijkerbuijk BMJM, Klein Gebbink RJM, Savenije TJ and Siebbeles. *J Am Chem Soc* 2008; **130**: 2485–2492.
24. Stubinger T and Brutting W. *J. Appl. Phys.* 2001; **90**: 3632–3641.
25. Hoppe H and Sariciftci NS. *J. Mater. Chem.* 2006; **16**: 45–61.
26. Chen S-G, Stradins P and Gregg BA. *J. Phys. Chem. B* 2005; **109**: 13451–13460.
27. Liu A, Zhao S, Rim S-B, Wu J, Könemann M, Erk P and Peumans P. *Adv. Mater.* 2008; **20**: 1065–1070.
28. Peumans P and Forrest SR. *Appl. Phys. Lett.* 2001; **79**: 126.
29. Xue J, Rand BP, Uchida S and Forrest SR. *Adv. Mater.* 2005; **17**: 66–71.
30. Dai JG, Jiang XX, Wang HB and Yan DH. *Appl. Phys. Lett.* 2007; **91**: 253503.
31. Yang F, Lunt RR and Forrest SR. *Appl. Phys. Lett.* 2008; **92**: 053310.
32. Bailey-Salzman RF, Rand BP and Forrest SR. *Appl. Phys. Lett.* 2007; **91**: 013508.
33. Brumbach M, Placencia D and Armstrong NR. *J. Phys. Chem. C* 2008; **112**: 3142–3151.
34. Varotto A, Nam C-Y, Radivojevic I, P. C. Tomé J, Cavaleiro JAS, Black CT and Drain CM. *J. Am. Chem. Soc.* 2010; **132**: 2552–2554.
35. Mutolo KL, Mayo EI, Rand BP, Forrest SR and Thompson ME. *J. Am. Chem. Soc.* 2006; **128**: 8108–8109.
36. Rajaputra S, Vallurupalli S and Singh VP. *J. Mater. Sci. – Mater. Electron.* 2007; **18**: 1147–1150.
37. Kim I, Haverinen HM, Wang Z, Madakuni S, Kim Y, Li J and Jabbour GE. *Chem. Mater.* 2009; **21**: 4256–4260.
38. Lessmann R, Hong Z, Scholz S, Maennig B, Riede MK and Leo K. *Org. Electron.* 2010; **11**: 539–543.
39. Koeppe R and Sariciftci NS. *Photochem. Photobiol. Sci.* 2006; **5**: 1122–1131.
40. Lungenschmied C, Dennler G, Neugebauer H, Sariciftci SN, Glatthaar M, Meyer T and Meyer A. *Sol. Energy Mater. Sol. Cells* 2007; **91**: 379–384.
41. Ameri T, Dennler G, Lungenschmied C and Brabec CJ. *Energy Environ. Sci.* 2009; **2**: 347–363.
42. Dennler G, Prall H-J, Koeppe R, Egginger M, Autengruber R and Sariciftci NS. *Appl. Phys. Lett.* 2006; **89**: 073502.
43. Janssen AGF, Riedl T, Hamwi S, Johannes HH and Kowalsky W. *Appl. Phys. Lett.* 2007; **91**: 073519.
44. Colsmann A, Junge J, Kayser C and Lemmer U. *Appl. Phys. Lett.* 2006; **89**: 203506.
45. Zhao DW, Tang WH, Ke L, Tan ST and Sun XW. *ACS Appl. Mater. Interfaces* 2010; **2**: 829–837.
46. Xue J, Uchida S, Rand BP and Forrest SR. *Appl. Phys. Lett.* 2004; **85**: 5757.
47. Maennig B, Drechsel J, Gebeyehu D, Simon P, Kozlowski F, Werner A, Li F, Grundmann S, Sonntag S, Koch M, Leo K, Pfeiffer M, Hoppe H, Meissner D, Sariciftci NS, Riedel I, Dyakonov V and Parisi J. *Appl. Phys. A Mater. Sci. Process.* 2004; **79**: 1–14.
48. Takahashi K, Nakamura J-I, Yamaguchi T, Komura T, Ito S and Murata K. *J. Phys. Chem. B* 1997; **101**: 991–997.
49. Takahashi K, Goda T, Yamaguchi T, Komura T and Murata K. *J. Phys. Chem. B* 1999; **103**: 4868–4875.
50. Takahashi K, Asano M, Imoto K, Yamaguchi T, Komura T, Nakamura J-I and Murata K. *J. Phys. Chem. B* 2003; **107**: 1646–1652.
51. Bhattacharya S, Ujihashi N, Aonuma S, Kimura T and Komatsu N. *Spectrochim. Acta, Part A* 2007; **68**: 495–503.
52. Guldi DM, Nuber B, Bracher PJ, Alabi CA, MacMahon S, Kukol JW, Wilson SR and Schuster DI. *J. Phys. Chem. A* 2003; **107**: 3215–3221.
53. Sanchez L, Sierra M, Martin N, Myles AJ, Dale TJ, Rebek J, Jr., Seitz W and Guldi DM. *Angew. Chem., Int. Ed.* 2006; **45**: 4637–4641.
54. Hasobe T, Imahori H, Fukuzumi S and Kamat PV. *J. Phys. Chem. B* 2003; **107**: 12105–12112.
55. Isosomppi M, Tkachenko NV, Efimov A, Kaunisto K, Hosomizu K, Imahori H and Lemmetyinen H. *J. Mater. Chem.* 2005; **15**: 4546–4554.
56. Fischer MKR, Lopez-Duarte I, Wienk MM, Martinez-Diaz MV, Janssen RAJ, Bauerle P and Torres T. *J. Am. Chem. Soc.* 2009; **131**: 8669–8676.
57. Oku T, Noma T, Suzuki A, Kikuchi K and Kikuchi S. *J. Phys. Chem. Solids* 2010; **71**: 551–555.
58. Liu C-Y, Pan H-L, Fox MA and Bard AJ. *Chem. Mater.* 1997; **9**: 1422–1429.
59. Schouten PG, Warman JM, de Haas MP, Fox MA and Pan H-L. *Nature* 1991; **353**: 736–737.
60. Gregg BA, Fox MA and Bard AJ. *J. Phys. Chem.* 1990; **94**: 1586–1598.
61. Liu C and Bard AJ. *J. Am. Chem. Soc.* 1998; **120**: 5575–5576.
62. Kang S-W, Li Q, Chapman BD, Pindak R, Cross JO, Li L, Nakata M and Kumar S. *Chem. Mater.* 2007; **19**: 5657–5663.
63. Zhou X, Kang S-W, Kumar S, Kulkarni RR, Cheng SZD and Li Q. *Chem. Mater.* 2008; **20**: 3551–3553.
64. Sandanayaka ASD, Murakami T and Hasobe T. *J. Phys. Chem. C* 2009; **113**: 18369–18378.

Copyright © 2010 World Scientific Publishing Company

65. Hasobe T, Imahori H, Kamat PV, Ahn TK, Kim SK, Kim D, Fujimoto A, Hirakawa T and Fukuzumi S. *J. Am. Chem. Soc.* 2005; **127**: 1216–1228.
66. Hasobe T, Imahori H, Kamat PV and Fukuzumi S. *J. Am. Chem. Soc.* 2003; **125**: 14962–14963.
67. Hasobe T. *Phys. Chem. Chem. Phys.* 2010; **12**: 44–57.
68. Jiang L and Li Y. *J. Porphyrins Phthalocyanines* 2007; **11**: 299–312.
69. Vail SA, Schuster DI, Guldi DM, Isosomppi M, Tkachenko N, Lemmetyinen H, Palkar A, Echegoyen L, Chen X and Zhang JZH. *J. Phys. Chem. B* 2006; **110**: 14155–14166.
70. Cho Y-J, Ahn TK, Song H, Kim KS, Lee CY, Seo WS, Lee K, Kim SK, Kim D and Park JT. *J. Am. Chem. Soc.* 2005; **127**: 2380–2381.
71. Tannert S, Ermilov EA, Vogel JO, Choi MTM, Ng DKP and Roder B. *J. Phys. Chem. B* 2007; **111**: 8053–8062.
72. Ermilov EA, Tannert S, Werncke T, Choi MTM, Ng DKP and Roeder B. *Chem. Phys.* 2006; **328**: 428–437.
73. D'Souza F, Chitta R, Gadde S, Rogers LM, Karr PA, Zandler ME, Sandanayaka ASD, Araki Y and Ito O. *Chem. Eur. J.* 2007; **13**: 916–922.
74. Ito F, Ishibashi Y, Khan SR, Miyasaka H, Kameyama K, Morisue M, Satake A, Ogawa K and Kobuke Y. *J. Phys. Chem. A* 2006; **110**: 12734–12742.
75. de la Escosura A, Martinez-Diaz MV, Guldi DM and Torres T. *J. Am. Chem. Soc.* 2006; **128**: 4112–4118.
76. El-Khouly ME, Araki Y, Ito O, Gadde S, McCarty AL, Karr PA, Zandler ME and D'Souza F. *Phys. Chem. Chem. Phys.* 2005; **7**: 3163–3171.
77. Gust D, Moore TA and Moore AL. *Acc. Chem. Res.* 2000; **34**: 40–48.
78. Durantini EN. *Synth. Commun.* 2006; **36**: 2135–2144.
79. D'Souza F, Smith PM, Zandler ME, McCarty AL, Itou M, Araki Y and Ito O. *J. Am. Chem. Soc.* 2004; **126**: 7898–7907.
80. Gonzalez-Rodriguez D and Bottari G. *J. Porphyrins Phthalocyanines* 2009; **13**: 624–636.
81. Kaunisto K, Vahasalo H, Chukharev V, Tkachenko NV, Vivo P, Niemi M, Tolkki A, Efimov A and Lemmetyinen H. *Thin Solid Films* 2009; **517**: 2988–2993.
82. Kaunisto K, Vuorinen T, Vahasalo H, Chukharev V, Tkachenko NV, Efimov A, Tolkki A, Lehtivuori H and Lemmetyinen H. *J. Phys. Chem. C* 2008; **112**: 10256–10265.
83. Imahori H, Kimura M, Hosomizu K, Sato T, Ahn TK, Kim SK, Kim D, Nishimura Y, Yamazaki I, Araki Y, Ito O and Fukuzumi S. *Chem. Eur. J.* 2004; **10**: 5111–5122.
84. Koeppe R, Sariciftci NS, Troshin PA and Lyubovskaya RN. *Appl. Phys. Lett.* 2005; **87**: 244102.
85. Hasobe T, Kamat PV, Absalom MA, Kashiwagi Y, Sly J, Crossley MJ, Hosomizu K, Imahori H and Fukuzumi S. *J. Phys. Chem. B* 2004; **108**: 12865–12872.
86. Yun J-J, Jung H-S, Kim S-H, Han E-M, Vaithianathan V and Jenekhe SA. *Appl. Phys. Lett.* 2005; **87**: 123102.
87. Dastoor PC, McNeill CR, Frohne H, Foster CJ, Dean B, Fell CJ, Belcher WJ, Campbell WM, Officer DL, Blake IM, Thordarson P, Crossley MJ, Hush NS and Reimers JR. *J. Phys. Chem. C* 2007; **111**: 15415–15426.
88. Burke KB, Belcher WJ, Thomsen L, Watts B, McNeill CR, Ade H and Dastoor PC. *Macromol.* 2009; **42**: 3098–3103.
89. Maree CHM, Roosendaal SJ, Savenije TJ, Schropp REI, Schaafsma TJ and Habraken FHPM. *J. Appl. Phys.* 1996; **80**: 3381–3389.
90. Savenije TJ, Koehorst RBM and Schaafsma TJ. *Chem. Phys. Lett.* 1995; **244**: 363–370.
91. Savenije TJ, Moons E, Boschloo GK, Goossens A and Schaafsma TJ. *Phys. Rev. B: Condens. Matter Mater. Phys.* 1997; **55**: 9685–9692.
92. Akiyama T, Matsushita M, Kakutani K, Yamada S, Takechi K, Shiga T, Motohiro T, Nakayama H and Kohama K. *Jpn. J. Appl. Phys., Part 1* 2005; **44**: 2799–2802.
93. Walter MG and Wamser CC. *Mat. Res. Soc. Symp. Proc.* 2007; **1013**: Z04–07.
94. Umeyama T, Takamatsu T, Tezuka N, Matano Y, Araki Y, Wada T, Yoshikawa O, Sagawa T, Yoshikawa S and Imahori H. *J. Phys. Chem. C* 2009; **113**: 10798–10806.
95. Liu Y, Guo X, Xiang N, Zhao B, Huang H, Li H, Shen P and Tan S. *J. Mater. Chem.* 2010; **20**: 1140–1146.
96. Hasobe T, Saito K, Kamat PV, Troiani V, Qiu H, Solladie N, Kim KS, Park JK, Kim D, D'Souza F and Fukuzumi S. *J. Mater. Chem.* 2007; **17**: 4160–4170.
97. O'Regan B and Grätzel M. *Nature* 1991; **353**: 737–740.
98. Bessho T, Zakeeruddin SM, Yeh C-Y, Diau EW-G and Grätzel M. *Angew. Chem. Int. Ed.* 2010; **49**: 6646–6649.
99. Kay A and Grätzel M. *J. Phys. Chem.* 1993; **97**: 6272–6277.
100. Kay A, Humphry-Baker R and Grätzel M. *J. Phys. Chem.* 1994; **98**: 952–959.
101. Wang X-F and Tamiaki H. *Energy Environ. Sci.* 2009; **3**: 94–106.
102. Imahori H, Umeyama T and Ito S. *Acc. Chem. Res.* 2009; **42**: 1809–1818.
103. Rio Y, Vazquez P and Palomares E. *J. Porphyrins Phthalocyanines* 2009; **13**: 645–651.
104. Campbell WM, Burrell AK, Officer DL and Jolley KW. *Coord. Chem. Rev.* 2004; **248**: 1363–1379.

Copyright © 2010 World Scientific Publishing Company

105. Cherian S and Wamser CC. *J. Phys. Chem. B* 2000; **104**: 3624–3629.
106. Jasieniak J, Johnston M and Waclawik ER. *J. Phys. Chem. B* 2004; **108**: 12962–12971.
107. Ma TL, Inoue K, Noma H, Yao K and Abe E. *J. Photochem. Photobiol., A* 2002; **152**: 207–212.
108. Meen TH, Water W, Chen WR, Chao SM, Ji LW and Huang CJ. *J. Phys. Chem. Solids* 2009; **70**: 472–476.
109. Odobel F, Blart E, Lagree M, Villieras M, Boujtita H, El Murr N, Caramori S and Alberto Bignozzi C. *J. Mater. Chem.* 2003; **13**: 502–510.
110. Trachibana Y, Haque SA, Mercer IP, Durrant JR and Klug DR. *J. Phys. Chem. B* 2000; **104**: 1198–1205.
111. Imahori H, Hayashi S, Hayashi H, Oguro A, Eu S, Umeyama T and Matano Y. *J. Phys. Chem. C* 2009; **113**: 18406–18413.
112. Imahori H, Hayashi S, Umeyama T, Eu S, Oguro A, Kang S, Matano Y, Shishido T, Ngamsinlapasathian S and Yoshikawa S. *Langmuir* 2006; **22**: 11405–11411.
113. Planells M, Forneli A, Martínez-Ferrero E, Sánchez-Díaz A, Sarmentero MA, Ballester P, Palomares E and O'Regan BC. *Appl. Phys. Lett.* 2008; **92**: 153506.
114. Rochford J, Chu D, Hagfeldt A and Galoppini E. *J. Am. Chem. Soc.* 2007; **129**: 4655–4665.
115. Boschloo GK and Goossens A. *J. Phys. Chem.* 1996; **100**: 19489–19494.
116. de Tacconi NR, Chanmanee W, Rajeshwar K, Rochford J and Galoppini E. *J. Phys. Chem. C* 2009; **113**: 2996–3006.
117. Galoppini E, Rochford J, Chen H, Saraf G, Lu Y, Hagfeldt A and Boschloo G. *J. Phys. Chem. B* 2006; **110**: 16159–16161.
118. Walter MG, Wamser CC, Ruwitch J, Zhao Y, Braden D, Stevens M, Denman A, Pi R, Rudine A and Pessiki PJ. *J. Porphyrins Phthalocyanines* 2007; **11**: 601–612.
119. Kim H-S and Wamser CC. *Photochem. Photobiol. Sci.* 2006; **5**: 955–960.
120. Lindsey JS. *Acc. Chem. Res.* 2009; **43**: 300–311.
121. Imahori H, Matsubara Y, Iijima H, Umeyama T, Matano Y, Ito S, Niemi M, Tkachenko NV and Lemmetyinen H. *J. Phys. Chem. C* 2010; **114**: 10656–10665.
122. Hayashi S, Tanaka M, Hayashi H, Eu S, Umeyama T, Matano Y, Araki Y and Imahori H. *J. Phys. Chem. C* 2008; **112**: 15576–15585.
123. Stromberg JR, Marton A, Kee HL, Kirmaier C, Diers JR, Muthiah C, Taniguchi M, Lindsey JS, Bocian DF, Meyer GJ and Holten D. *J. Phys. Chem. C* 2007; **111**: 15464–15478.
124. Lu H-P, Mai C-L, Tsia C-Y, Hsu S-J, Hsieh C-P, Chiu C-L, Yeh C-Y and Diau EW-G. *Phys. Chem. Chem. Phys.* 2009; **11**: 10270–10274.
125. Lu H-P, Tsai C-Y, Yen W-N, Hsieh C-P, Lee C-W, Yeh C-Y and Diau EW-G. *J. Phys. Chem. C* 2009; **113**: 20990–20997.
126. Nazeeruddin MK, De Angelis F, Fantacci S, Selloni A, Viscardi G, Liska P, Ito S, Takeru B and Grätzel M. *J. Am. Chem. Soc.* 2005; **127**: 16835–16847.
127. Nazeeruddin MK, Pechy P, Renouard T, Zakeeruddin SM, Humphry-Baker R, Comte P, Liska P, Cevey L, Costa E, Shklover V, Spiccia L, Deacon GB, Bignozzi CA and Grätzel M. *J. Am. Chem. Soc.* 2001; **123**: 1613–1624.
128. Jensen RA, Van Ryswyk H, She C, Szarko JM, Chen LX and Hupp JT. *Langmuir* 2009; **26**: 1401–1404.
129. Lee CY and Hupp JT. *Langmuir* 2009; **26**: 3760–3765.
130. Hsieh C-P, Lu H-P, Chiu C-L, Lee C-W, Chuang S-H, Mai C-L, Yen W-N, Hsu S-J, Diau EW-G and Yeh C-Y. *J. Mater. Chem.* 2010; **20**: 1127–1134.
131. Mai C-L, Huang W-K, Lu H-P, Lee C-W, Chiu C-L, Liang Y-R, Diau EW-G and Yeh C-Y. *Chem. Commun.* 2010; **46**: 809–811.
132. Chang C-W, Luo L, Chou C-K, Lo C-F, Lin C-Y, Hung C-S, Lee Y-P and Diau EW-G. *J. Phys. Chem. C* 2009; **113**: 11524–11531.
133. Lin C-Y, Lo C-F, Luo L, Lu H-P, Hung C-S and Diau EW-G. *J. Phys. Chem. C* 2009; **113**: 755–764.
134. Lin C-Y, Wang Y-C, Hsu S-J, Lo C-F and Diau EW-G. *J. Phys. Chem. C* 2010; **114**: 687–693.
135. Luo L, Lin C-J, Tsai C-Y, Wu H-P, Li L-L, Lo C-F, Lin C-Y and Diau EW-G. *Phys. Chem. Chem. Phys.* 2010; **12**: 1064–1071.
136. Eu S, Hayashi S, Umeyama T, Oguro A, Kawasaki M, Kadota N, Matano Y and Imahori H. *J. Phys. Chem. C* 2007; **111**: 3528–3537.
137. Liu Y, Xiang N, Feng X, Shen P, Zhou W, Weng C, Zhao B and Tan S. *Chem. Commun.* 2009: 2499–2501.
138. Mozer AJ, Griffith MJ, Tsekouras G, Wagner P, Wallace GG, Mori S, Sunahara K, Miyashita M, Earles JC, Gordon KC, Du L, Katoh R, Furube A and Officer DL. *J. Am. Chem. Soc.* 2009; **131**: 15621–15623.
139. Giribabu L, Kumar CV and Reddy PY. *J. Porphyrins Phthalocyanines* 2006; **10**: 1007–1016.
140. Giribabu L, Vijay Kumar C, Raghavender M, Somaiah K, Reddy P and Venkateswara Rao P. *J. Chem. Sci.* 2008; **120**: 455–462.
141. Nazeeruddin MK, Humphry-Baker R, Officer DL, Campbell WM, Burrell AK and Grätzel M. *Langmuir* 2004; **20**: 6514–6517.
142. Campbell WM, Jolley KW, Wagner P, Wagner K, Walsh PJ, Gordon KC, Schmidt-Mende L, Nazeeruddin MK, Wang Q, Grätzel M and Officer DL. *J. Phys. Chem. C* 2007; **111**: 11760–11762.
143. Wang Q, Campbell WM, Bonfantani EE, Jolley KW, Officer DL, Walsh PJ, Gordon K, Humphry-Baker R,

Copyright © 2010 World Scientific Publishing Company

Nazeeruddin MK and Grätzel M. *J. Phys. Chem. B* 2005; **109**: 15397–15409.
144. Allegrucci A, Lewcenko NA, Mozer AJ, Dennany L, Wagner P, Officer DL, Sunahara K, Mori S and Spiccia L. *Energy Environ. Sci.* 2009; **2**: 1069–1073.
145. Armel V, Pringle JM, Forsyth M, MacFarlane DR, Officer DL and Wagner P. *Chem. Commun.* 2010; **46**: 3146–3148.
146. Mozer AJ, Wagner P, Officer DL, Wallace GG, Campbell WM, Miyashita M, Sunahara K and Mori S. *Chem. Commun.* 2008: 4741–4743.
147. Santos TD, Morandeira A, Koops S, Mozer AJ, Tsekouras G, Dong Y, Wagner P, Wallace G, Earles JC, Gordon KC, Officer D and Durrant JR. *J. Phys. Chem. C* 2010; **114**: 3276–3279.
148. Eu S, Hayashi S, Umeyama T, Matano Y, Araki Y and Imahori H. *J. Phys. Chem. C* 2008; **112**: 4396–4405.
149. Park JK, Chen J, Lee HR, Park SW, Shinokubo H, Osuka A and Kim D. *J. Phys. Chem. C* 2009; **113**: 21956–21963.
150. Brumbach MT, Boal AK and Wheeler DR. *Langmuir* 2009; **25**: 10685–10690.
151. Cho TJ, Shreiner CD, Hwang S-H, Moorefield CN, Courneya B, Godinez LA, Manriquez J, Jeong K-U, Cheng SZD and Newkome GR. *Chem. Commun.* 2007: 4456–4458.
152. Fukuzumi S, Hasobe T, Ohkubo K, Crossley MJ, Kamat PV and Imahori H. *J. Porphyrins Phthalocyanines* 2004; **8**: 191–200.
153. Imahori H and Umeyama T. *J. Phys. Chem. C* 2009; **113**: 9029–9039.
154. Zhang DS and Xiao XR. *Chin. Chem. Lett.* 2000; **11**: 813–814.
155. Kang MS, Oh JB, Roh SG, Kim MR, Lee JK, Jin SH and Kim HK. *Bull. Korean Chem. Soc.* 2007; **28**: 33–40.
156. Amao Y and Komori T. *Biosens. Bioelectron.* 2004; **19**: 843–847.
157. Amao Y and Yamada Y. *Langmuir* 2005; **21**: 3008–3012.
158. Tsurumoto T, Toyoda M and Amao Y. *Colloids Surf., A* 2006; **284–285**: 623–626.
159. Amao Y and Yamada Y. *Biosens. Bioelectron.* 2007; **22**: 1561–1565.
160. Ikegami M, Ozeki M, Kijitori Y and Miyasaka T. *Electrochem. (Tokyo, Jpn.)* 2008; **76**: 140–143.
161. Wang XF, Matsuda A, Koyama Y, Nagae H, Sasaki S, Tamiaki H and Wada Y. *Chem. Phys. Lett.* 2006; **423**: 470–475.
162. Wang X-F, Koyama Y, Nagae H, Wada Y, Sasaki S-I and Tamiaki H. *J. Phys. Chem. C* 2008; **112**: 4418–4426.
163. Wang X-F, Tamiaki H, Wang L, Tamai N, Kitao O, Zhou H and Sasaki S-I. *Langmuir* 2010; **26**: 6320–6327.
164. Wang X-F, Kitao O, Zhou H, Tamiaki H and Sasaki S-I. *Chem. Commun.* 2009: 1523–1525.
165. Wang X-F, Kitao O, Zhou H, Tamiaki H and Sasaki S-I. *J. Phys. Chem. C* 2009; **113**: 7954–7961.
166. Cid J-J, Garcia-Iglesias M, Yum J-H, Forneli A, Albero J, Martinez-Ferrero E, Vazquez P, Grätzel M, Nazeeruddin MK, Palomares E and Torres T. *Chem. Eur. J.* 2009; **15**: 5130–5137.
167. Silvestri F, Garcia-Iglesias M, Yum J-H, Vazquez P, Martinez-Diaz MV, Grätzel M, Nazeeruddin MK and Torres T. *J. Porphyrins Phthalocyanines* 2009; **13**: 369–375.
168. Eu S, Katoh T, Umeyama T, Matano Y and Imahori H. *Dalton Trans.* 2008: 5476–5483.
169. Amao Y and Komori T. *Langmuir* 2003; **19**: 8872–8875.
170. Komori T and Amao Y. *J. Porphyrins Phthalocyanines* 2003; **7**: 131–136.
171. Chou C-S, Yanga R-Y, Weng M-H and Yeh C-H. *Mater. Sci. Forum* 2008; **594**: 281–298.
172. Chou C-S, Yang R-Y, Weng M-H and Yeh C-H. *Powder Technol.* 2008; **187**: 181–189.
173. Chuen-Shii C, Ru-Yuan Y, Min-Hang W and Chun-Hung Y. *Adv. Powder Technol.* 2008; **19**: 541–558.
174. Cid J-J, Yum J-H, Jang S-R, Nazeeruddin MK, Martinez-Ferrero E, Palomares E, Ko J, Grätzel M and Torres T. *Angew. Chem., Int. Ed.* 2007; **46**: 8358–8362.
175. Yum JH, Jang SR, Humphry-Baker R, Grätzel M, Cid JJ, Torres T and Nazeeruddin MK. *Langmuir* 2008; **24**: 5636–5640.
176. Balraju P, Kumar M, Roy MS and Sharma GD. *Synth. Met.* 2009; **159**: 1325–1331.
177. Reddy PY, Giribabu L, Lyness C, Snaith HJ, Vijaykumar C, Chandrasekharam M, Lakshmikantam M, Yum JH, Kalyanasundaram K, Grätzel M and Nazeeruddin MK. *Angew. Chem. Int. Ed.* 2007; **46**: 373–376.
178. Mori S, Nagata M, Nakahata Y, Yasuta K, Goto R, Kimura M and Taya M. *J. Am. Chem. Soc.* 2010; **132**: 4054–4055.
179. He J, Benko G, Korodi F, Polivka T, Lomoth R, Akermark B, Sun L, Hagfeldt A and Sundstrom V. *J. Am. Chem. Soc.* 2002; **124**: 4922–4932.
180. Morandeira A, Lopez-Duarte I, Martinez-Diaz MV, O'Regan B, Shuttle C, Haji-Zainulabidin NA, Torres T, Palomares E and Durrant JR. *J. Am. Chem. Soc.* 2007; **129**: 9250–9251.
181. O'Regan BC, Lopez-Duarte I, Martinez-Diaz MV, Forneli A, Albero J, Morandeira A, Palomares E, Torres T and Durrant JR. *J. Am. Chem. Soc.* 2008; **130**: 2906–2907.
182. Palomares E, Martinez-Diaz MV, Haque SA, Torres T and Durrant JR. *Chem. Commun.* 2004: 2112–2113.

Copyright © 2010 World Scientific Publishing Company

183. Rawling T, Austin C, Buchholz F, Colbran SB and McDonagh AM. *Inorg. Chem.* 2009; **48**: 3215–3227.
184. Walker D, Chappel S, Mahammed A, Brunschwig BS, Winkler JR, Gray HB, Zaban A and Gross Z. *J. Porphyrins Phthalocyanines* 2006; **10**: 1259–1262.
185. Aviv I and Gross Z. *Chem. Commun.* 2007: 1987–1999.
186. Saltsman I, Goldberg I and Gross Z. *Tetrahedron Lett.* 2003; **44**: 5669–5673.
187. Balanay MP, Dipaling CVP, Lee SH, Kim DH and Lee KH. *Sol. Energy Mater. Sol Cells* 2007; **91**: 1775–1781.
188. Balanay MP and Kim DH. *Phys. Chem. Chem. Phys.* 2008; **10**: 5121–5127.
189. Ma R, Guo P, Cui H, Zhang X, Nazeeruddin MK and Grätzel M. *J. Phys. Chem. A* 2009; **113**: 10119–10124.
190. Ma R, Guo P, Yang L, Guo L, Zhang X, Nazeeruddin MK and Grätzel M. *J. Phys. Chem A* 2010; **114**: 1973–1979.
191. Ma R, Guo P, Yang L, Guo L, Zeng Q, Liu G and Zhang X. *Theochem* 2010; **942**: 131–136.
192. Mor GK, Shankar K, Paulose M, Varghese OK and Grimes CA. *Nano Lett.* 2006; **6**: 215–218.
193. Meen T-H, Huang C-J, Chen Y-W, Ji L-W, Diao C-C and Chung H-H. *Key Eng. Mater.* 2008; **368–372**: 1716–1719.

Copyright © 2010 World Scientific Publishing Company